



HAL
open science

Role of the supplementary motor area during reproduction of supra-second time intervals: An intracerebral EEG study

Micha Pfeuty, Vincent Monfort, Madelyne Klein, Julien Krieg, Steffie Collé,
Sophie Colnat-Coulbois, H el ene Brissart, Louis Maillard

► To cite this version:

Micha Pfeuty, Vincent Monfort, Madelyne Klein, Julien Krieg, Steffie Coll e, et al.. Role of the supplementary motor area during reproduction of supra-second time intervals: An intracerebral EEG study. *NeuroImage*, 2019, 191, pp.403-420. 10.1016/j.neuroimage.2019.01.047 . hal-02056381

HAL Id: hal-02056381

<https://hal.science/hal-02056381>

Submitted on 22 Oct 2021

HAL is a multi-disciplinary open access archive for the deposit and dissemination of scientific research documents, whether they are published or not. The documents may come from teaching and research institutions in France or abroad, or from public or private research centers.

L'archive ouverte pluridisciplinaire **HAL**, est destin ee au d ep ot et  a la diffusion de documents scientifiques de niveau recherche, publi es ou non,  emanant des  tablissements d'enseignement et de recherche fran ais ou  trangers, des laboratoires publics ou priv es.



Distributed under a Creative Commons Attribution - NonCommercial 4.0 International License

Role of the Supplementary Motor Area during Reproduction of Supra-Second Time Intervals: an Intracerebral EEG Study

Micha Pfeuty*¹, Vincent Monfort*², Madelyne²Klein, Julien Krieg^{3,4}, Steffie Collé², Sophie Colnat-Coulbois^{3,4}, H el ene Brissart^{3,4}, Louis Maillard^{3,4,5,6}

¹University of Bordeaux, INCIA, UMR 5287, F-33000 Bordeaux, France.

²University of Lorraine, 2LPN, EA 7489 Rue du G en eral Delestraint, Metz, F-57070, France.

³Universit e de Lorraine, CRAN, UMR 7039, Campus Sciences, Boulevard des Aiguillettes, 54500 Vandoeuvre-l es-Nancy, France

⁴CNRS, CRAN, UMR 7039, Campus Sciences, Boulevard des Aiguillettes, 54500 Vandoeuvre-l es-Nancy, France

⁵University Hospital of Nancy, Department of Neurology, 29 avenue du Mar chal-de-Lattre-de-Tassigny, Nancy, F-54035, France.

⁶Facult e de M edecine de Nancy, Universit e de Lorraine, 9 Avenue de la For t de Haye, 54500 Vandoeuvre-l es-Nancy, France

*Both authors equally contributed to this work

Corresponding author:

Vincent Monfort: University of Lorraine, 2LPN, EA 7489, Rue du G en eral Delestraint, Metz, F-57070, France.

Abstract

The supplementary motor area (SMA) has been shown to be involved in interval timing but its precise role remains a matter of debate. The present study was aimed at examining, by means of intracerebral EEG recordings, the time course of the activity in this structure, as well as in other functionally connected cortical (frontal, cingulate, insular and temporal) areas, during a visual time reproduction task. Four patients undergoing stereo-electroencephalography (SEEG) for presurgical investigation of refractory focal epilepsy were enrolled. They were selected on the presence of depth electrodes implanted within the SMA. They were instructed to encode, keep in memory and then reproduce the duration (3, 5 and 7 s) of emotionally-neutral or negative pictures. Emotional stimuli were used with the aim of examining neural correlates of temporal distortions induced by emotion. Event-related potentials (ERPs) were analyzed during three periods: During and at the extinction of the target interval (TI) and at the beginning of the reproduction interval (RI). Electrophysiological data revealed an ERP time-locked to TI-offset whose amplitude varied monotonically with TI-duration. This effect was observed in three out of the four patients, especially within the SMA and the insula. It also involved the middle and anterior cingulate cortex, the superior, middle and inferior frontal gyri and the paracentral lobule. These effects were modulated by the prior TI-duration and predicted variations in temporal reproduction accuracy. In contrast, modulations of ERPs with TI-duration, emotion or temporal performance during the target or the reproduction interval were modest and less consistent across patients. These results demonstrate that, during reproduction of supra-second time intervals, the SMA, in concert with a fronto-insular network, is involved at the end of the target interval, and suggest a role in the duration categorization and decision making operations or alternatively in the preparedness of the timing of the future movement that will be executed during the reproduction phase.

Keywords: Time perception; Stereoelectroencephalography; Supplementary motor area; Insular cortex; Frontal cortex; Duration encoding.

1. Introduction

The ability to perceive the passage of time is essential for individuals to adapt to a changing environment. Numerous studies aiming at elucidating the neurobiological basis of time perception in the milliseconds to seconds range (i.e., interval timing) presuppose the existence of a dedicated clock in the brain and are based on the “pacemaker-accumulator” model (Gibbon, 1977). According to this information-processing model, pulses are emitted by an oscillatory pacemaker with a certain frequency and gathered into an “accumulator” via a “switch” (controlled by attention) that closes and opens at the onset and the offset of the to-be-timed event, respectively. The content of the accumulator indexing the perceived event duration is stored transiently in a working memory system and/or permanently in a reference memory system. Finally, a decision mechanism compares the current duration values with those in reference memory to perform an adequate behavior.

Neuroimaging and neuropsychological studies have suggested that interval timing mechanisms are distributed in the brain and could rely on a large network including the cerebellum, the basal ganglia as well as the frontal, parietal and temporal cortices. It has been proposed that the engagement of each specific brain region could depend on the duration range (seconds or sub-seconds), the sensory modality (visual, auditory, tactile or multimodal) or the nature (perceptual or sensori-motor) of the task at hand (Ivry and Spencer, 2004; Lewis and Miall, 2003; Merchant et al., 2013). Interestingly, a review of functional magnetic resonance imaging (fMRI) studies by Wiener et al. (2010) using a conjunction analysis pointed the supplementary motor area (SMA) and the right inferior frontal gyrus (IFG) as the only structures consistently activated irrespective of a specific timing context.

Great attention has been given to the SMA which, in connection with the striatum, might provide the neural substrate of the accumulation process commonly postulated in models of time processing (Pouthas et al., 2005). This putative role is supported by a high

number of fMRI studies showing that SMA activity during timing perceptive task increases with physical duration (Pouthas et al., 2005; Wencil et al., 2010), perceived duration (Tipples et al., 2013), or the amount of attention allocated to the duration of stimulus (Coull et al., 2004; Henry et al., 2015; Hermann et al., 2014). Furthermore, Coull et al. (2015) suggested that SMA selectively codes the accumulation of temporal magnitude by showing that its activity increased incrementally as a function of both physical and perceived duration, but not as function of distance. This role of SMA in temporal accumulation is also in line with single-cell recordings in monkeys showing increasing SMA activity as a function of duration during temporal prediction (Akkal et al., 2004), or reproduction of single (Mita et al., 2009) or multiple intervals (Merchant et al., 2013). Similarly, scalp EEG studies in humans have shown that the amplitude of the contingent negative variation (CNV), a slow negative potential usually recorded over medial frontal electrodes and supposed to originate from the SMA (Gomez et al., 2003; Kononowicz et al., 2015; Mento et al., 2013), varies in line with the perceived duration (Macar and Vidal, 2002). When physically identical target durations are compared to a previously memorized standard, a larger negativity is associated to a longer duration judgment (Bendixen et al., 2005; Macar et al., 1999). This pattern of results suggests that the level of activation for the subjectively longer durations is relatively high as compared to the pre-defined level stored in reference memory and provides a strong argument that the CNV indexes the accumulation process (Macar et al., 1999).

However, other empirical findings raise questions on the exact process that is reflected by the CNV recorded during the to-be-timed interval (Kononowicz et al., 2016; Van Rijn et al., 2011, for review). Using a time production procedure, the seminal work by Macar and colleagues (1999) has shown that larger CNV amplitudes are observed when the target duration is over-produced, which seems to be at odds with the construct of temporal accumulation. Indeed, if a higher level of negativity reflects an accelerated accumulation of

pulses, one can predict that the threshold value corresponding to the target duration is reached earlier (Van Rijn et al., 2011). High-amplitude CNV trials are thus supposed to be associated with a response that occurred before the target duration and not afterwards. Interestingly, in reproduction tasks for which a number of different target intervals were used, the amplitude of the CNV recorded during the reproduction phase has been found to be negatively correlated with the duration of the target interval, a finding which appears to be inconsistent with an accumulation account (Elbert et al., 1991; Kononowicz et al., 2015). In addition, larger amplitude of both the early (initial CNV: iCNV) and late (late CNV: lCNV) components of the CNV during the reproduction phase has also been associated with underproduction of intervals and this effect was more pronounced for the shorter reproduction interval (Kononowicz et al., 2015). From these results, Kononowicz and colleagues (2015) proposed that the negative relationship between temporal estimates and iCNV amplitude is likely to reflect preparatory and anticipatory processes initiated right after the beginning of the reproduced interval and suggested that the preparation level is larger for the shorter target interval (Kononowicz et al., 2015).

The challenge in establishing the factors on which the link between CNV and time processing depends is emphasized by recent electrophysiological studies that have failed to find any performance-related effects on the CNV amplitude in similar motor timing tasks (Kononowicz and Van Rijn, 2011; Tamm et al., 2014; Kononowicz et al., 2016, for review). Moreover, some studies demonstrated that the subjective timing of supra-second time intervals was better reflected by EEG activity occurring at the beginning of the interval (Kononowicz et al., 2015; Kononowicz and Van Rijn, 2015) or by post-interval ERPs that follow the CNV resolution (i.e. amplitude of N1-P2 complex; Kononowicz and Van Rijn, 2014a). In the context of a time production task, in which a motor response is generated, higher beta power measured at the onset of the to-be-timed interval appears to be associated

with overproduced durations (Kononowicz and Van Rijn, 2015). Among the post-duration ERPs, the N1-P2 complex varies according to the magnitude of difference between target and comparison intervals (Kononowicz and Van Rijn, 2014a) and the late positive component of timing (LPCt) is modulated with the difficulty of temporal decision (i.e. when spacing between comparison intervals is reduced; Paul et al., 2011) or with physical duration (Gontier et al., 2009; Lindbergh and Kieffaber, 2013). Collectively, these electrophysiological studies indicated that at least some timing mechanisms continue after the offset of the to-be-timed stimulus and questioned the role of climbing neural activity in the subjective timing, as indexed by the CNV (Kononowicz et al., 2016, for review).

Finally, fMRI studies found an activity resembling to an accumulation process in the middle (Buetti and Macaluso, 2011) and posterior (Wittmann et al., 2010) parts of the insula but not in the SMA during the encoding phase of temporal reproduction tasks. This activity would be followed by the activation of a frontal network encompassing the pre-SMA and the anterior insular cortex/inferior frontal gyrus (AIC/IFG) during the reproduction phase, suggesting that SMA is not involved in the accumulation process. Preparatory processes to an upcoming stimulus (Kononowicz and Van Rijn, 2014a), motor inhibition (Coull et al., 2016; Kononowicz and Van Rijn, 2015), keeping a representation of the target interval during the reproduction phase (Wittmann et al., 2010), or general cognitive effort irrespective of whether the task requires to process temporal information or not (Livesey et al., 2007) have been considered as alternative proposals to describe the role of the SMA in interval timing.

Stereo-electroencephalographic (SEEG) recordings offer a unique opportunity to explore the time course of activity in targeted cortical brain regions thus making possible precise measures of where and when activity occurs in the brain. To date, there has been no attempt to examine the neural correlates of time perception by means of this technique. Given the putative role of SMA in the build-up and in the keeping of a representation of a time

interval, the aim of the present study was to investigate the temporal dynamics of intracerebral EEG activity in this brain region during the encoding, the retention and the reproduction of time intervals. Considering the hypothesis of a “temporal hub” with a distributed network of brain structures (Merchant et al., 2013, for review), activity was also examined in the other implanted brain regions. The task was similar to that used by Wittmann et al. (2010) or by Kononowicz et al. (2015). Participants were presented a target interval (TI: 3, 5 and 7 s) they had to encode, to keep in memory, and then to reproduce. In order to bias the subjective perception of time, emotionally-negative pictures known to induce distortion of temporal judgment (Droit-Volet and Meck, 2007, for review) and neutral pictures were presented during the encoding phase. This task was presented to four subjects with drug-refractory epilepsy who had intracerebral electrodes implanted in the SMA. Because a putative neural accumulator located in the SMA is supposed to be involved during the coding and retrieval of a target interval (Coull et al., 2008), we predicted that the amplitude of the **CNV-like activity** recorded in the SMA during the encoding and reproduction phases correlates with the subjective duration (i.e. with trial-to-trial fluctuations of temporal performance), and also with temporal distortions induced by emotion. Within this conceptual framework, we expected that the amplitude of the **CNV-like activity** evoked by the target interval (TI) and the reproduction interval (RI) should increase and decrease, respectively, when participants over-produced temporal intervals. Alternatively, if SMA activity locked to the onset of the RI reflects motor preparation and expectation, higher amplitude of the **CNV-like activity** should be associated with both the short TI-duration (i.e. 3s interval; Elbert et al., 1991; Gibbons & Rammsayer, 2004; Kononowicz et al., 2015) and under-produced intervals (Kononowicz et al., 2015). Under the assumption that temporal processing continues after TI-offset, we predicted that the brain responses recorded **during** the retention phase would be modulated according to the length of TI-duration and temporal performance.

2. Material and methods

2.1. Patients and electrodes implantation

Four patients (one female, mean age \pm SD: 32.0 \pm 13.8 years) with drug-refractory epilepsy and undergoing stereo-electroencephalographic (SEEG) evaluation of possible surgical intervention participated to the study. SEEG recording was performed in order to define the epileptogenic zone (Talairach and Bancaud, 1973). The choice of electrode location was based on pre-SEEG clinical and video-EEG recordings and made independently of the present study. Thus, each patient had a unique combination of recording sites. This study did not add any invasive procedure to depth EEG recordings. Inclusion criterion was the presence of intracerebral electrodes located in the SMA. An extensive description of brain structures explored by intracerebral electrodes is given in Table 1. The four patients had from 9 to 15 intracerebral electrodes stereotaxically implanted. Each electrode had a diameter of 0.8 mm and contained from 5 to 17 contiguous contacts of 2 mm in length separated by 1.5 mm (Dixi Medical, Besançon, France). Detailed information on the electrode implantation procedure can be found in Jonas et al. (2014). One patient presented a brain lesion identified by structural MRI and one patient presented a cortical dysplasia identified by SEEG investigation. All patients were fully informed about the aim of investigation before providing written consent for this study. They had normal or corrected-to-normal vision and they underwent neuropsychological assessment with evaluations of global efficiency, working memory, episodic memory, executive functions.

Insert Table 1 here

2.2. SEEG recordings

Intracerebral recordings were conducted using a video SEEG monitoring system that allowed the simultaneous recording of 128 SEEG channels (2 SD LTM 64 Headbox; Micromed, Italy) sampled at 512 Hz (0.15 – 250 Hz bandwidth; time constant = 1.06 s) during the experimental paradigm. One of the contact sites in the white matter was chosen as a reference. However, all signals were re-referenced to their nearest neighbor on the same electrode, 3.5 mm away before analysis (bipolar montage).

2.3. Experimental paradigm

We used a temporal reproduction task including two sessions of around 25 minutes that were performed successively separated by a 10-min pause. Each session was made of 5 blocks of 15 trials. There were a total of 150 trials, divided up into 25 trials for each combination of duration (3, 5 and 7 s) and emotion (neutral, negative). The different types of trials were presented in a pseudo-random order. Stimulus presentation and response collection were controlled via E-prime (PST - Psychology Software Tools, Pittsburgh, PA, USA).

Each trial began with the presentation of a picture for a target interval (TI) of 3, 5 or 7 s that the participants had to memorize. After a constant delay of 3500 ms, the reproduction interval (RI) started with the onset of a gray square on the screen. The participants had to press a button when they judge the duration of the gray square as equal to the memorized TI. If no button press occurred within a delay equal to 2.5 times the TI (7.5, 12.5 or 17.5 s), the gray square disappeared and the trial was counted as a missed trial (Figure 1).

Insert Figure 1 here (full width)

We used one hundred and fifty pictures from the International Affective Pictures System (IAPS; Lang et al., 2008) rated from 1 to 9 on the arousal and valence scales.

Seventy-five pictures were unpleasant with high arousal and low valence (mean arousal 6.05, mean valence 2.81) and seventy-five pictures were neutral with low arousal and intermediate valence (mean arousal 3.16, mean valence 5.01).

Not a single subject had seizures within the 12h before the reproduction task administration. The participants performed a training block (10 trials) before each session. A feedback (“too short”, “too long” or “correct”) was given after each training trial to inform the participants on their performance. The performance was considered as “correct” when the reproduction interval (RI) was less than 35% shorter or longer than the TI. No feedback was given during test trials.

2.4. Behavioral data analysis

The accuracy of temporal estimation was examined by computing for each patient, each TI and each emotion a *RI/TI ratio*. Since the TI was considered as the reference, a *RI/TI ratio* <1 (or > 1) corresponds to a *RI* shorter (or longer) than the TI. The precision of temporal reproduction was also examined by computing for each participant, each TI and each emotion, the coefficient of variation (*CV*) with the following formula: Standard Deviation (RI) / Mean (RI).

For each patient, a one-way ANOVA using linear contrasts with TI-duration (3, 5, 7 s) as a between-groups factor were first performed to determine whether the reproduction task was well executed, i.e. whether *RI* increased with TI-duration. Then, a two-way ANOVA with TI-duration (3, 5, 7 s) and Emotion (neutral, negative) as between-groups factors were performed to determine whether the *RI/TI ratio* was influenced by TI-duration and by emotion. The Bonferroni correction was applied for post-hoc comparisons.

2.5. Intracerebral ERP preprocessing

577 sites were recorded in 4 subjects with an average of 144 sites recorded simultaneously per patient (Table 1). There were a total of 390 bipolar derivations with an average of 97 per patient. Each electrode contact was located in one of the eight following regions: The supplementary motor area (SMA proper and pre-SMA), the superior frontal gyrus (SFG, outside of SMA), the middle frontal gyrus (MFG), the inferior frontal gyrus (IFG), the orbitofrontal cortex (OFC), the paracentral lobule (PCL), the middle and anterior cingulate cortex (MCC/ACC), the insular cortex (IC) and the extra-frontal regions (including temporal, parietal and occipital cortices, hippocampus and amygdala). Few contacts were outside the brain and were not taken into account. To determine if an electrode contact was located within the SMA, we used the most restricted boundaries of the mesial premotor cortex reported in the meta-analysis of functional neuroimaging studies by Mayka et al. (2006). Lateral, caudal, rostral and ventral boundaries were at $x = \pm 15$ mm, $y = -12$ mm, $y = 0$ mm and $z = 44$ mm for SMA proper and at $x = \pm 15$ mm, $y = 0$ mm, $y = 12$ mm and $z = 40$ mm for pre-SMA. Localization of the contacts outside the SMA was identified by Talairach Daemon (<http://www.talairach.org/daemon.html>) and Anatomical Automatic Labelling parcellation (AAL, Tzourio-Mazoyer et al., 2002). On this basis, there were 37 contacts (7%) in the SMA/pSMA, 113 (21%) in the SFG, 83 (15%) in the MFG, 25 (5%) in the IFG, 32 (6%) in the OFC, 45 (8%) in the PCL, 85 (15%) in the MCC/ACC, 20 (4%) in the IC and 111 electrodes (20%) in extra-frontal regions.

Event-related potentials (ERPs) were computed off-line using a combination of scripts and routines implemented in the EEGLAB v6.03b toolbox (Delorme and Makeig, 2002) for each bipolar derivation. We focused on the SEEG activity recorded during the to-be-timed periods, i.e. during encoding (ERPs time-locked to TI-onset) and reproduction (ERPs time-

locked to RI-onset) and also at the end of the encoding period (ERPs time-locked to TI-offset).

In classical EEG experiments, when S1-S2 intervals are longer than 1 s, the contingent negative variation (CNV) is generally made of two components, an early component developing between 200 and 1000 ms after S1, and a late component developing before S2 (Loveless and Sanford, 1974). For ERPs time-locked to TI-onset, analyses were performed on both the early (iCNV-like between 0.2 and 1 s) and the late (lCNV-like between 1 s and TI-offset) activity. For ERPs time-locked to TI-offset, analyses were performed over the whole retention period (between 0.2 and 3 s). Finally, for the reproduction period, analyses were performed only on the iCNV-like activity (between 0.2 and 1 s) as the later activity was influenced by motor response. For each bipolar derivation selected for statistical analyses (see next section), a visual inspection of the SEEG trials was performed and enabled the rejection of trials with interictal activities or artifacts.

2.6. Intracerebral ERP statistical analyses

2.6.1. ERPs time-locked to TI-onset

Because the patients were not informed about which TI-duration would be presented at each trial, no effect of TI-duration (3, 5, 7 s) was expected for ERPs time-locked to TI-onset. Analyses were first performed on the early (iCNV-like) activity (between 0.2 and 1 s). Two time windows were defined (tw1: 200-600ms, tw2: 600-1000ms) and the average voltage between -400 and 0 ms preceding TI-onset was used as baseline. We investigated whether the amplitude of the iCNV-like activity time-locked to TI-onset was affected by emotion and whether these effects could be related to the impact of emotion on time estimation. The mean amplitude of the iCNV-like activity time-locked to TI-onset was computed separately for the

trials associated with each emotion (neutral, negative). For each patient, the derivations in which visual inspection revealed an iCNV-like activity whose amplitude varied with emotion were selected for statistical analyses. Then, one-way ANOVAs with Emotion (neutral, negative) as between-group factor were performed separately for each selected derivation and each time window. We also investigated whether the amplitude of the iCNV-like activity time-locked to TI-onset reflected the accuracy in temporal estimation. The 150 trials were sorted into four quartiles (Q1, Q2, Q3, Q4) on the basis of the *RI/TI ratio*. The first (Q1) and fourth (Q4) quartiles correspond to the shortest and longest *RI/TI ratio*, respectively, while the second (Q2) and third (Q3) quartiles correspond to the *RI/TI ratio* just below and above the median, respectively. Because the *RI/TI ratio* generally decreases as a function of TI-duration (Lejeune & Wearden, 2009; Vierordt, 1869), this would lead to a higher number of 7s-TI trials in the first quartile and a higher number of 3s-TI trials in the fourth quartile. Therefore, a sorting was first performed separately for each TI-duration in order to have an equal number of trials for each TI-duration per quartile. For each TI-duration, there were 13 trials for quartiles Q1 and Q4, and 12 trials for quartiles Q2 and Q3, respectively. Afterwards, trials of the same quartile were pooled together across durations with a total of 39 trials for quartiles Q1 and Q4 and 36 trials for quartiles Q2 and Q3. Then, the mean amplitude of ERPs time-locked to TI-onset was calculated for the derivations in which visual inspection revealed an iCNV-like activity varying depending on the *RI/TI ratio*. One-way ANOVAs with linear contrasts using *RI/TI ratio* (quartiles Q1, Q2, Q3, Q4) as between-group factor were performed separately for each derivation and each time window.

Analyses were also performed on the late (iCNV-like) activity (between 1 s and TI-offset) in order to test whether a monotonically increasing or decreasing activity could be observed. The derivations in which visual inspection revealed an activity varying monotonically between 1 and 3 s following TI-onset for each TI-duration were selected for

statistical analyses. Five time windows were defined (tw1: 1000-1400ms, tw2: 1400-1800ms, tw3: 1800-2200ms, tw4: 2200-2600ms, tw5: 2600-3000ms) and the average voltage between -400 and 0 ms preceding TI-onset was used as baseline. A slope (s_{1-3}) was calculated between tw1 and tw5 and one sample t-tests were performed to determine whether it differed from zero. In this case, we tested whether the activity continued to increase or decrease between 3 and 5 s following TI-onset for the 5s-TI and the 7s-TI. Five time windows (tw6: 3000-3400ms, tw7: 3400-3800ms, tw8: 3800-4200ms, tw9: 4200-4600ms, tw10: 4600-5000ms) allowed to calculate a slope (s_{3-5}) and one sample t-tests were performed to determine whether it differed from zero and was in the same direction as s_{1-3} . Finally, for the derivations in which s_{1-3} and s_{3-5} had the same sign and were different from zero, we tested whether the activity continued to increase or decrease between 5 and 7 s following TI-onset for the 7s-TI. Five time windows (tw11: 5000-5400ms, tw12: 5400-5800ms, tw13: 5800-6200ms, tw14: 6200-6600ms, tw15: 6600-7000ms) allowed to calculate a slope (s_{5-7}) and one sample t-tests were performed to determine whether it differed from zero and was in the same direction as s_{1-3} and s_{3-5} .

2.6.2. ERPs time-locked to TI-offset

The EEG was segmented into epochs starting 400 ms before and ending 3000 ms after TI-offset. Seven time windows were defined (tw1: 200-600ms, tw2: 600-1000ms, tw3: 1000-1400ms, tw4: 1400-1800ms, tw5: 1800-2200ms, tw6: 2200-2600ms, tw7: 2600-3000ms) and the average voltage between -400 and 0 ms preceding TI-offset was used as baseline. For each patient, the derivations in which visual inspection revealed the presence of ERPs time-locked to TI-offset whose amplitude varied with TI-duration, emotion or *RI/TI ratio* were selected for statistical analyses. Then, one-way ANOVAs using linear contrasts were performed separately for each selected derivation and each time window, with TI-duration (3, 5 and 7 s)

or *RI/TI ratio* (quartiles Q1, Q2, Q3, Q4) as between-group factor. One-way ANOVAs with Emotion (neutral, negative) as between-group factor were also carried out for each selected derivation and each time window.

2.6.3. ERPs time-locked to RI-onset

The analyses were performed on the iCNV-like activity (between 0.2 and 1 s) following RI-onset. Two time windows were defined (tw1: 200-600ms, tw2: 600-1000ms) and the average voltage between -400 and 0 ms preceding RI-onset was used as baseline. For each patient, the derivations in which visual inspection revealed an iCNV-like activity varying depending on the TI-duration or the *RI/TI ratio* were selected for statistical analyses. Then, one-way ANOVAs using linear contrasts with TI-duration (3, 5 and 7 s) or *RI/TI ratio* (quartiles Q1, Q2, Q3, Q4) as between-group factor were performed separately for each selected derivation and each time window.

2.6.4. Statistical procedure

For each one-way ANOVA, a correction was applied when the Levene test failed to confirm the homogeneity of variance of ERP data. Furthermore, a Bonferroni correction was applied for conducting analyses in multiple time windows ($p < .05/\text{number of time windows}$). The Bonferroni correction was also applied for post-hoc comparisons. For the derivations in which statistical analyses revealed a significant effect of TI-duration, emotion or *RI/TI ratio* on ERPs, Brodmann areas and corresponding gyri were identified by Talairach Daemon and AAL (<http://www.talairach.org/daemon.html>; Tzourio-Mazoyer et al., 2002).

3. Results

3.1. Behavioral results

For all patients except patient 1, *RI* significantly increased with TI-duration, the 5s-TI being reproduced significantly longer than the 3s-TI and significantly shorter than the 7s-TI (patients 2, 3 and 4: $t > 12.79$, $p < .001$ and Bonferroni-corrected $p < .001$ for all post-hoc t-tests, patient 1: $t(146) = 1.86$, $p = .06$ and Bonferroni-corrected $p > .10$ for all post-hoc t-tests; see Figure 2-a, Tables S1-a and S1-b). Therefore, the task was well-executed by all patients, except by patient 1. Furthermore, the effect sizes (Cohen's d ; Table S1-b) were significantly larger in patient 3, indicating better discrimination between each TI-duration than in the other patients as illustrated in Figure 3.

Insert Figure 2 here (single column)

The two-way ANOVA performed to test individually the effect of TI-duration and Emotion on the *RI/TI ratio* revealed a main effect of TI-duration for all patients except patient 3 (Figure 2-b) and no main or interaction effect of Emotion (Tables S1-a and S1-c). In all patients except patient 3, the *RI/TI ratio* decreased with TI-duration and was significantly larger for the 3s-TI than for the 7s-TI, a pattern of results in line with Vierordt's law (Lejeune & Wearden, 2009; Vierordt, 1869).

Insert Figure 3 here (full width)

3.2. ERPs results

3.2.1. ERPs time-locked to TI-onset

The early (iCNV-like) activity following TI-onset was modulated by emotion only in patient 2 on one derivation located in the AIC (Table 2-a, Figure S1-a). The presence of ERPs varying

linearly with *RI/TI ratio* was also observed only in patient 3 on two derivations located in the SFG and IFG (Table 2-b, Figure S1-b).

Insert Table 2 here

During the late activity period, an increasing or decreasing activity between 1 and 3 s was observed on 4 derivations in patient 1, 15 derivations in patients 2, 10 derivations in patients 3 and 18 derivations in patients 4. When we tested for the 5s-TI and the 7s-TI whether the activity continues to increase or decrease between 3 and 5 s, two derivations located in the SMA (patient 1 and 3), and one derivation located in the SFG (patient 4) and two derivations located in the PCL (patient 4), revealed a slope s_{3-5} different from zero and in the same direction as slope s_{1-3} . For these five derivations, the slope s_{5-7} measured for the 7s-TI was not significantly different from zero (Figure 4). For the derivations in which the ICNV-like activity varied continuously between 1 and 5 s, we tested whether the slope between 1 and 3 s (s_{1-3}) or the mean amplitude between 1 and 3 s (m_{1-3}) were modulated by emotion or by *RI/TI ratio*. The one-way ANOVAs with Emotion (neutral, negative) as between-group factor and the one-way ANOVAs with linear contrast using *RI/TI ratio* (quartiles Q1, Q2, Q3, Q4) as between-group factor did not reveal any significant effect for s_{1-3} and m_{1-3} .

Insert Figure 4 (single column)

3.2.2. ERPs time-locked to TI-offset

The activity following TI-offset was modulated by TI-duration in three patients (patients 2, 3 and 4). ANOVAs with linear contrasts indicated that ERPs time-locked to TI-offset varied significantly in amplitude with TI-duration on a total of 42 bipolar derivations (Table 3, Figures 5 and 6). Bonferroni post-hoc comparisons revealed differences in ERPs amplitude

between the 3s-TI and the 7s-TI in all the cases, between the 3s-TI and the 5s-TI in 29% of cases and between the 5s-TI and the 7s-TI in 26% of cases. The effect was observed within the SMA (SMA proper and pre-SMA), the insular cortex (anterior and posterior), the middle frontal gyrus (MFG) and the middle and anterior cingulate cortex (MCC/ACC) in the three patients, within the inferior and superior frontal gyri (IFG, SFG) in two patients (patients 3 and 4), within the orbitofrontal cortex (OFC) and the hippocampus (H) only in patient 2, and within the paracentral lobule (PCL) only in patient 4 (Figure 7). A χ^2 test revealed that the number of contacts showing a modulation of ERPs amplitude with TI-duration (relatively to the number of electrode contacts) differed between brain regions ($\chi^2 = 43.6$, $df = 8$, $p < .001$). The ratio of electrode contacts showing an effect was higher into the insula (8/20, 40%) and the SMA/pSMA (13/37, 35%) than in the other regions (Figure 8). The modulations of ERPs amplitude with TI-duration were observed between 200 and 3000 ms after TI-offset but the time-course of the effect differed between brain regions ($\chi^2 = 82.1$, $df = 48$, $p < .001$, Table 4). Although effects were globally observed on the whole retention period, most of the effects were observed over earlier time-windows (TW1 and TW2) in the SFG and MFG, and over later time-windows (TW3, TW4 and TW5) in the SMA/pSMA and ACC/MCC.

Insert Tables 3 & 4, Figures 5 (full width), 6a (full width) & 6b (full width) here

ERPs time-locked to TI-offset were modulated by emotion only in patient 3 on one derivations located in the SFG (Table 5-a, Figure S2-a). The presence of ERPs varying linearly with *RI/TI ratio* was observed only in patient 4 on one derivation located in the MCC (Table 5-b, Figure S2-b).

Insert Table 5, Figures 7 (single column) & 8 (single column) here

3.2.3. ERPs time-locked to RI-onset

The early (iCNV-like) activity following RI-onset was modulated by TI-duration in two patients (patients 3 and 4) on a total of four derivations located within the MFG in the two patients and in the PCL only in patient 4 (Table 6 and Figure S3-a). Bonferroni post-hoc comparisons revealed differences in ERPs amplitude between the 3s-TI and the 7s-TI in all the cases but not between the 3s-TI and the 5s-TI nor between the 5s-TI and the 7s-TI (Table 6 and Figure S3-a). The presence of ERPs varying linearly with *RI/TI ratio* was also observed in two patients (Patients 3 and 4) on a total of four derivations located in the MFG and MCC in the patient 3 and in the pSMA and the IFG in the patient 4 (Table 7 and Figure S3-b).

Insert Tables 6 & 7 here

3.2.4. ERPs time-locked to TI-offset: Evolution of the TI-duration effects across the duration of the experiment

The most consistent result revealed by the present study was the presence of ERPs time-locked to TI-offset whose amplitude was modulated by TI-duration. Further analyses were performed to examine whether the effect could be due to habituation to the temporal context and would arise in the course of the experiment. The 150 trials (50 trials per duration) were split in two parts of 75 trials (P1 for the first 75 trials and P2 for the last 75 trials). Then, for each bipolar derivation and each time window in which the amplitude of ERPs was significantly modulated by TI-duration, one-way ANOVAs using linear contrasts with TI-duration as a between-groups factor were performed separately for each part of the experiment (Table S2). The total number of electrode contacts with a significant effect of TI-duration (using a $p < .05$ level of significance) did not significantly differ between the two parts of the experiments ($\chi^2 = 0.9$, $df = 1$, $p > .10$). However, as shown in Figure S4, the ratio of electrode contacts showing an effect was higher into the insular cortex than in the other brain regions in P1 (8/20, 40%, $\chi^2 = 19.1$, $df = 1$, $p < .001$) but not in P2 (4/20, 20%, $\chi^2 = 1.9$,

df = 1, $p > .10$). By contrast, the ratio of electrode contacts showing an effect was higher into the SMA than in the other brain regions in P2 (13/37, 35%, $\chi^2 = 24.8$, df = 1, $p < .001$) but not in P1 (6/37, 13%, $\chi^2 = 1.4$, df = 1, $p > .10$).

3.2.5. ERPs time-locked to TI-offset: Modulation by the TI-duration presented in the prior trial

The presence of ERPs time-locked to TI-offset whose amplitude was modulated by TI-duration suggests that this post-interval activity could reflect temporal categorization of the TI-duration in comparison to an expected duration based on the temporal context. However, the value of this expected duration could vary from trials to trials depending on the previous TI-duration. The amplitude of post-interval ERPs has actually been shown to vary with the duration presented in the prior trial (Wiener & Thompson, 2015) and longer (shorter) prior intervals lead to shorter (longer) perceived durations (Wiener et al., 2014). If the temporal context indeed impacts the ERPs time-locked to TI-offset, the magnitude of the TI-duration presented in the prior trial should predict the amplitude of this post-interval activity.

To test this assumption, a visual inspection of the averaged waveforms was first performed for the 42 bipolar derivations in which post-interval activity was shown to vary linearly with TI-duration. This enabled us to distinguish two patterns of post-interval activity modulated by TI-duration depending on the derivation: (1) a phasic activity consisting of two peaks, a negativity (or positivity) followed by a positive (or negative) deflection, with a shorter TI-duration associated with a larger peak-to-peak difference, or (2) a tonic activity consisting in a sustained activity modulated by TI-duration. The pattern was considered as phasic on 24 derivations (0 in patient 2, 18 in patient 3 and 6 in patient 4), and tonic on 18

derivations (8 in patient 1, 3 in patient 3 and 7 in patient 4). For derivations in which the pattern of post-interval activity modulated by TI-duration was phasic, we calculated a phasic activity index (mean amplitude of the 400ms time windows corresponding to the positive peak minus mean amplitude of the 400ms time windows corresponding to the negative peak). For derivations in which the pattern of post-interval activity modulated by TI-duration was tonic, we calculated a tonic activity index (mean amplitude over the successive 400ms time windows revealing a significant effect of TI-duration).

Simple regression analyses were first conducted. They confirmed for the 42 bipolar derivations that TI-duration was a significant predictor of the phasic or tonic activity index (Table S3-a). It is of note that in all cases, a shorter TI-duration predicted a larger phasic activity index (the regression coefficient was negative). Then, multiple regression analyses were carried out to determine whether the phasic or tonic activity index was also predicted by the TI-duration presented in the prior trial. In our experiment, each TI-duration had higher probability to be preceded by a different rather than by the same TI-duration. Thus, there was a negative correlation between the TI-duration presented in the current trial and the TI-duration presented in the prior trial. Therefore, TI-duration in the current trial and TI-duration in the prior trial were both entered as predictors of the phasic or tonic activity index. TI-duration in the prior trial was shown to be a significant predictor of the phasic or tonic activity index in the three patients on a total of nine bipolar derivations located in the MCC in two patients (patients 2 and 3), in the OFC only in patient 2, in the pSMA, SFG, MFG and IFG only in patient 3, and in the PCL only in patient 4 (Table S3-b). In all but one case, the signs of the regression coefficients were opposite for the TI-duration in the current trial (Table S3-a) and the TI-duration in the prior trial (Table S3-b). This indicates that when post-interval activity index was predicted by shorter TI-duration in the current trial, it was also predicted by longer TI-duration in the prior trial, in line with an impact of the temporal context on the post-

interval activity (Figure S5-a). This suggests that, when the prior TI-duration was longer, the current TI-duration was categorized as shorter and thus, should have been under-produced. However, we did not observe any effect of the prior TI-duration on the temporal reproduction accuracy. This could be due to an opposite bias linked to the reproduction time of the precedent trial. In line with this assumption, partial regression analyses revealed that, in patients 1, 2 and 4, the reproduction time in the current trial was positively associated with the reproduction time in the prior trial, when corrected for the current and the prior TI-duration (patient 1: $r = .35$, $p < .001$; patient 2: $r = .22$, $p = .011$; patient 4: $r = .35$, $p < .001$).

3.2.6. ERPs time-locked to TI-offset: Prediction of the temporal reproduction performance

ERPs time-locked to TI-offset were modulated by TI-duration in each patient except patient 1 who was the only patient who was not able to correctly perform the reproduction task. This suggests that this post-interval activity could predict the temporal reproduction performance. Although previous ANOVAs revealed that ERPs time-locked to TI-offset varying linearly with *RI/TI ratio* only in patient 4 on one derivation located in the MCC (section 3.2.2), new regression analyses were performed on the 42 bipolar derivations in which post-interval activity was shown to vary linearly with TI-duration. We used the phasic and tonic activity indexes calculated in the previous section (3.2.5). The aim was to determine whether this post-interval index was a key predictor of the magnitude of the reproduction interval (*RI*) and of the accuracy of temporal estimation (*RI/TI ratio*).

Simple regression analyses were first conducted on the 42 derivations to determine whether the phasic or tonic activity index was a significant predictor of the reproduction interval (*RI*). The phasic or the tonic activity occurring after the extinction of the target interval predicted the magnitude of the reproduction interval (*RI*) in the three patients on a

total of 38 derivations (Table S4-a). In all cases, the sign of the regression coefficient between TI-duration and the post-interval activity index (Table S3-a) had the same direction as the sign of the regression coefficient between the post-interval activity index and *RI* (Table S4-a). This indicates that when a shorter TI-duration predicted a larger post-interval activity, a larger post-interval activity in turn predicted a shorter reproduction interval.

Then, for these 38 derivations, further regression analyses were conducted to determine whether the phasic or tonic activity index was also a significant predictor of the accuracy of temporal estimation (*RI/TI* ratio). In line with Vierordt's law, the *RI/TI* ratio decreased with TI-duration in patients 2 and 4 (Figure 3). For these patients, multiple regression analyses were performed in which the post-interval activity index and the TI-duration were entered as predictors and the *RI/TI* ratio was entered as the dependent variable. For the patient 3, in whom no central tendency effect was observed (Figure 3), simple regression analyses were conducted in which the post-interval activity index was entered as unique predictor. The post-interval activity index was shown to be a significant predictor of the *RI/TI* ratio in the three patients on a total of six bipolar derivations located in the SMA in two patients (patients 2 and 3), in the MCC in patient 3, and in the PCL in patient 4 (Table S4-b). In all cases, the sign of the regression coefficient between TI-duration and the post-interval activity index (Table S3-a) had the same direction as the sign of the regression coefficient between the post-interval activity index and the *RI/TI* ratio (Table S4-b). This indicates that when a shorter TI-duration predicted a larger post-interval activity, a larger post-interval activity in turn predicted a shorter *RI/TI* ratio (Figure S5-b).

3.2.7. *Late activity time-locked to the 7s-TI: Modulation by the TI-duration presented in the prior trial*

During the presentation of the 7s-TI, we observed on five derivations a late activity which varied monotonically until 5 s and then returned to baseline. This activity could reflect the expected duration based on the temporal context serving for the duration categorization process and may thus depend on the prior trial. We notably expected smaller CNV-like activity and more rapid return to baseline after a shorter TI-duration as observed in a previous EEG study using a bisection task (Wiener & Thompson, 2015). Then, for the five derivations, we tested whether the slope or the mean amplitude between 1 and 5 s (s1-5 and m1-5) and between 5 and 7 s (s5-7 and m5-7) were modulated by the TI-duration presented in the prior trial. Simple regression analyses revealed in one derivation in patient 4 located in the PCL that the slope of the activity between 1 and 5 s as well as the amplitude of the activity between 5 and 7 s were more positive when the prior TI-duration was longer (s1-5, $p = .008$; m5-7, $p = .020$). In another derivation in patient 4 located in the SFG, the slope between 5 and 7 s was more positive (s5-7: $p=.031$) when the prior TI-duration was shorter, indicating a more rapid return to baseline (Figure S6).

4. Discussion

The present study constitutes the first attempt to investigate, by means of intracerebral EEG recordings, the neural correlates of time perception. The SEEG activity was investigated in four epileptic patients within the SMA, as well as in other functionally connected cortical (notably frontal, cingulate and insular) regions while they performed a visual time reproduction task. The patients had to encode, keep in memory and then reproduce the duration (3, 5 and 7 s) of emotionally-neutral or negative pictures. Our aim was to determine whether the ERPs varied in amplitude according to the duration of target interval (at the extinction of the target interval and at the beginning of the reproduction), to the emotion of target stimulus (during and at the extinction of the target interval) and to the intra-individual

variations of temporal accuracy (at the beginning and at the extinction of the target interval and at the beginning of the reproduction interval).

The most consistent finding in the current study was that ERPs occurring at the offset of the target interval varied linearly with the TI-duration. This result was observed in three out of the four patients within the SMA/pSMA as well as in insular, frontal and cingulate regions. Further analyses revealed that, in several locations, this post-interval activity was predicted by the TI-duration presented in the prior trial and predicted the inter-trial variations in temporal reproduction accuracy. Less consistent evidence was found for the effects of TI-duration and of temporal performance on ERPs time-locked to the onset of the reproduction interval. Similarly, performance-based variations in the activity measured at the beginning of the target interval (iCNV-like) were only observed in one patient on two different locations. Furthermore, a late (iCNV-like) activity varying monotonically during the presentation of the target interval was observed within the SMA and other frontal medial frontal regions. However, no relationship was established between this ‘climbing’ activity and the performance in temporal reproduction. Finally, emotional stimuli did not have any effect on the temporal performance and only modest effects of emotion were observed on the ERPs time-locked to TI-onset and to TI-offset.

4.1. ERPs time-locked to TI-offset varying with TI-duration and with temporal performance

We observed ERPs at the end of the target interval whose amplitude varied linearly with TI-duration. This effect was primarily located within the insular cortex (anterior and posterior), the SMA (SMA proper and pre-SMA). These two regions were involved in three out of the four patients and the ratio of electrode contacts showing the effect was 40% (8/20) in the insula and 35 % (13/35) in the SMA/pSMA. The effect was also observed within the middle

and anterior cingulate cortex (MCC/ACC), the superior, middle and inferior frontal gyri (SFG, MFG and IFG), the paracentral lobule (PCL), the orbitofrontal cortex (OFC) and the hippocampus (H). This modulation of post-interval ERPs with the duration of target interval occurred from 200 to 3000 ms following the TI-offset but different time courses were observed according to the brain region. The SFG and MFG were mainly engaged during earlier time windows (200 to 1000 ms), whereas the SMA/pSMA and the MCC/ACC were more importantly involved during later time-windows (1000 to 2200 ms).

The fact that this effect was not limited to early time-windows and was especially frequent on derivations localized into frontal, insular and cingulate cortical areas argues against a low order visual response such as an “off” signal or a rebound effect which is usually found in the retina and visual areas (Duysens et al., 1996). It is also noteworthy that among the four patients, patient 1 was the only one who did not manage to differentiate the three target interval durations (Figures 2 and 3) and whose SMA activity at TI-offset was not modulated by TI-duration (Figure 5). By contrast, ERPs time-locked to TI-offset showed the most acute effect of TI-duration for the patient 3 (Figures 5 and 6), who had also the best ability to differentiate the three target interval durations (Figures 2 and 3). Therefore, the specific pattern of neuronal activity and the temporal individual performance obtained for these two patients suggest that the modulation of post-interval ERPs with TI-duration does not simply reflect implicit processing of TI-duration and could be associated with mechanisms that contribute to an explicit and accurate representation of the target interval duration. This idea is reinforced by the fact that ERPs time-locked to TI-offset predicted the magnitude of the reproduction interval for most of the derivations showing an effect of TI-duration and also predicted the accuracy of temporal estimation in several of these derivations.

Interestingly, the effects of the TI-duration on the ERPs time-locked to TI-offset were observed on two different patterns of post-interval activity: a phasic activity consisting of a

negativity (or positivity) followed by a positivity (or negativity), and a tonic activity consisting in a sustained activity whose amplitude was modulated by TI-duration. The pattern of the post-interval activity modulated by TI-duration was phasic on 24 derivations and tonic on 18 derivations. Shorter TI-duration was associated with larger phasic post-interval activity (peak-to-peak difference). By contrast, no particular assumption could be formulated about the direction of the relationship between the TI-duration and the tonic post-interval activity. Actually, because tonic post-interval activity consisted in a sustained activity in opposite directions for the shortest and the longest TI-duration, one could not determine whether the higher level of activity was associated to the shorter or longer TI-duration. Hence, the functional interpretation of this pattern of activity remains ambiguous and could equally correspond to memory storage mechanisms with activity increasing with the length of the interval to be remembered (Ng et al., 2009) or to motor preparation with higher level of activity when patients reproduced the 3s TI interval (Kononowicz et al., 2015). It is of note that, in patient 4, a ‘climbing’ activity was observed during the target interval in several derivations in which the tonic post-interval activity was modulated by the TI-duration (X1-X2, M2-M3 and P4-P5). However, for the 7s-TI, the slope of this climbing activity decreased after 5 s (central TI-duration). Thus, the modulations of the tonic post-interval activity with TI-duration observed on these derivations could actually reflect differences in the slope of the ICNV-like activity just before the TI-offset.

In a large number of derivations, the phasic post-interval activity was shown to be larger at the extinction of a shorter TI-duration. A first hypothesis is that this signal may be related with a post-interval component termed the late positive component of timing (LPCt) that prior scalp ERP studies observed immediately following the comparison interval in temporal discrimination (Tarantino et al., 2010; Gontier et al., 2009), generalization (Paul et al., 2011) or bisection (Wiener & Thompson, 2015; Lindberg & Kieffaber, 2013) tasks. Some

of these studies showed that the amplitude of the LPCt scaled linearly depending on the objective or subjective durations that had just been presented, with larger positive amplitudes at fronto-central sites for the shorter durations (Wiener & Thompson, 2015; Lindberg & Kieffaber, 2012; Tarantino et al., 2010). This pattern of brain activity was associated with a decrease of mean reaction times from short to long comparison intervals in a temporal discrimination task (Tarantino et al., 2010) and with faster response times for “long” responses relative to “short” responses in a temporal bisection task (Lindberg & Kieffaber, 2012). The decrease in the amplitude of post-interval activity with TI-duration in the present study is reminiscent of these previous findings and similarly indicates that decision regarding the temporal interval may be consistently time-locked to stimulus offset for the shortest durations, while the main part of the decision has been processed before the end of the longest durations (Lindberg & Kieffaber, 2012; Tarantino et al., 2010). Our results would not only confirm that this specific pattern activity reflects the neural signature of temporal categorization and decision-making operations but, in addition, reveal that this brain response depends on a network involving primarily the SMA and the insula and occurs immediately following the encoding of the TI-duration even though no response is required, as is the case following a comparison interval in temporal discrimination or bisection tasks. These data support previous single-cell electrophysiological findings that neurons in the frontal cortex (Genovesio et al., 2009) or the basal ganglia (Chiba et al., 2008) are active at the extinction of S1 in a timing task in which monkeys have to discriminate the duration of two successive stimuli S1 and S2. Genovesio et al. (2009) notably found that the level of post-interval activity in substantial populations of frontal neurons correlated positively (climbing activity) or negatively (declining activity) with S1 duration. Of particular note, a recent study using single-cell recording in the primate pre-SMA found category-selective neurons whose activity predicts the future categorical choice made by the animal in a bisection temporal task

(Mendoza et al., 2018). More importantly, the cells that were associated with the short category selection increased their activity after the presentation of the test interval whereas the neurons associated with the long category selection showed increased activity before the test interval offset. The larger post-interval activity observed in the SMA and in functionally connected cortical regions at the extinction of shorter TI-duration is consistent with these different findings showing that post-interval activity predicts the categorical decision and that long intervals are categorized as soon as the elapsed time exceeds the subjective boundary between short and long intervals (Mendoza et al., 2018).

Previous neuroimaging studies also indicate that the SMA plays a role in temporal predictability (Cui et al., 2009; Buetti et al., 2010). In a cued reaction-time task, Cui et al. (2009) observed that the activation of the SMA measured at the moment of the target appearance increased with the duration of a variable and uncertain foreperiod. Strikingly, this effect was no longer observed in a countdown condition in which the arrival time of the target was known in advance, suggesting that the cumulative conditional probability of the target occurrence rather than elapsed time was coded by SMA activity. Analogously, TI-durations are variable and uncertain in the present study but, contrary to Cui et al.'s (2009) findings, the SMA activity was shown to decrease with increasing probability of TI-offset. In both temporal reproduction and cued reaction-time tasks, expectancy depends on a posteriori probability distribution called the "hazard function", namely the increasing conditional probability over time that an event (i.e. the end of the target duration or the end of the readiness period) will occur given that it has not already occurred (Luce, 1986; Coull, 2009). In these tasks, an uncertainty is generated by the fact that the target duration in the current trial is not known in advance. But, since time always flows forward, the conditional probability increases inexorably over time so that the more time lapses, the more the uncertainty about the duration of the currently presented target interval decreases and the

more the expectation rises. However, the differences in terms of post-interval activity in the SMA could rely on the specific requirements of each task. Participants in the study by Cui et al. (2009) had to take a motor decision immediately after the target appearance whereas in our study, at the ending of the target interval, the patients had to keep a representation of the TI-duration in memory in order to anticipate the precise moment of the future button press that will be executed in the reproduction period. We tentatively propose that declining activity in the SMA in the present study codes for decision-making mechanisms build upon the decrease of uncertainty while climbing SMA activity reported by Cui et al (2009) could instead index the increase of temporal expectation with foreperiod duration. Considering that uncertainty about the duration of the current interval is maximal before the end of the 3s-TI, the higher amplitude of ERPs time-locked to the end of the shortest TI-duration may thus reflect the fact that the resolution of the uncertainty is at its height. Consistent with this explanation, the LPCt immediately following the end of to-be-timed interval has recently been considered as an electrophysiological marker of decision uncertainty during temporal processing (Wiener & Thompson, 2015).

Assuming that the decrease of SMA activity with TI-duration is associated with learned temporal expectations about the probability of TI-offset, this effect should be more important as the patient is habituated to the experimental context, and thus be more pronounced in the second than in the first part of the experiment. We did not find any significant increase in the number of derivations with a significant effect of TI-duration between the first and second parts of the experiment. However, in comparison with other brain regions, the ratio of derivations with a significant effect of TI-duration was higher into the insular cortex in the first part of the experiment whereas it was higher into the SMA in the second part of the experiment. This suggests that the modulation of post-interval activity with TI-duration increased in the SMA across the duration of the experiment and thus could reflect

increased knowledge of temporal expectation due to habituation to the experimental context. By contrast, the modulation of post-interval activity with TI-duration observed in the insular cortex decreased in the course of the experiment and could be involved in the explicit representation of the time interval which would shift progressively towards a more implicit representation.

If the post-interval activity reflects categorization of the TI-duration in comparison to an expected duration, we assumed that the value of this expected duration should vary from trials to trials depending on the TI-duration presented in the prior trial. We notably expected that if post-interval activity increases (or decreases) when the TI-duration presented in the current trial is shorter, it should similarly increase (or decrease) when the TI-duration presented in the prior trial is longer. Such carryover effects were actually observed on several derivations located in different brain regions, indicating that the post-interval effects were influenced by the temporal context. However, the magnitude of the reproduction interval was also expected to be shorter after a longer prior TI-duration. Yet, no effect of the prior TI-duration on the temporal reproduction accuracy was observed. However, complementary analyses revealed that this perceptual influence of the prior TI-duration would be compensated by an opposite bias according to which time intervals are more likely reproduced similarly to the preceding trial in line with a previous study revealing a similar decisional effect during a bisection temporal task (Wiener et al., 2014).

These modulations of post-interval ERPs were primarily observed within the pre-SMA and SMA proper and insular cortex. It also involved cingulate, middle frontal, inferior frontal and premotor cortical regions which are known to be functionally and/or structurally connected to the SMA/pSMA and/or the insula. The frontal aslant tract (FAT) has been shown to connect the SMA/pSMA with the IFG and a system of short U-shaped fibers interconnects the SFG, MFG and IFG (Catani et al., 2012). Besides, resting-state fMRI studies revealed that

the insula is functionally connected to the ACC in its anterior part and to the MCC and the SMA proper in its posterior part (Cauda et al., 2011; Deen et al., 2011; Taylor et al., 2009). A recent study investigating the connectivity of the frontal and insular regions using cortico-cortical evoked potential (CCEP) revealed connectivity between SMA/pSMA, insula, ventrolateral and dorsolateral premotor cortex (vPMC and dPMC), ACC and OFC (Enatsu et al., 2016). Interestingly, connections were mainly observed from the dPMC, vPMC and insula in the direction of the SMA/pSMA which could explain that, in our study, the modulations of ERPs occurring at the extinction of the encoding stimulus were mainly limited to the early post-interval period within the premotor (Brodmann area 6) while they continued for a longer period within the SMA/pSMA.

4.2. ERPs time-locked to RI-onset varying with TI-duration and with temporal performance

In a recent EEG/MEG study by Kononowicz et al. (2015) using reproduction of 2, 3 and 4 s target intervals, the amplitude of the CNV activity occurring at the beginning (between 300 and 600 ms) of the reproduction period was shown to decrease with TI-duration. Furthermore, the CNV amplitude was also shown to correlate with inter-individual variations of the *RI/TI ratio*. Based on these results, they suggested that the EEG activity occurring at the beginning of the reproduction period (i.e. corresponding to the early CNV) would reflect preparedness and anticipation of the precise moment of the future button press that will be executed to reproduce the TI-duration. Higher level of preparedness and of anticipation would be required for the reproduction of shorter TI-durations and conversely, for a given TI-duration, would result in shorter *RI/TI ratios*. In the present study, the ERPs time-locked to the beginning of reproduction interval revealed a similar effect (Figure S1) but it was observed in only two patients on a total of four derivations located in middle frontal gyrus (MFG) and the

paracentral lobule (PCL). The ERPs time-locked to RI-onset were also shown to vary linearly with *RI/TI ratio* in two patients in the MFG, IFG, pre-SMA and MCC regions. However, no CNV was clearly observed and it is not clear whether these differences were related to more activity for shorter or for longer TI-durations. Nonetheless, Kononowicz et al. (2015) suggested that these preparedness and anticipation processes could actually occur before the reproduction period. We propose that the higher activity observed into a network encompassing the SMA and the insula after the offset of shorter TI-duration could reflect a higher level of preparedness and anticipation that is helpful to be optimally prepared for a decision at a certain point in time (i.e. pressing the button at the right moment in time). This would be in line with an fMRI study revealing that the activity within a network including the SMA and the right insula increased several seconds prior to self-initiated movements (Sakata et al., 2017) as well as with another study showing that slow intrinsic hemodynamic fluctuations within the SMA and insula are related to the moment at which a subject freely decide to press a key (Pfurtscheller et al., 2014).

4.3. ERPs time-locked to TI-onset varying with temporal performance

No consistent evidence was found at the beginning of the TI-onset regarding the presence of iCNV-like activity whose amplitude varied linearly with RI/TI ratio. This effect was observed in only one patient in the SFG and IFG regions making difficult to conclude about modulations of this early activity with trial-to-trial fluctuations of temporal judgment. Within the SMA (2 patients), the PCL (1 patient) and the SFG (1 patient) regions, an increasing or decreasing activity was observed between 1 and 3 s following TI-onset for each TI and also between 3 and 5 s for the 5s-TI and the 7s-TI during the temporal windows corresponding to the late CNV. However, for the 7s-TI, the ICNV-like activity stopped increasing or decreasing between 5 and 7 s. In previous scalp EEG studies using duration

discrimination tasks, CNV activity has been shown to peak at the end of the memorized rather than to the current duration (Macar and Vidal, 2003, Pfeuty et al., 2005) suggesting that it could reflect the expected duration. Such pattern of activity was also observed in an EEG study using a temporal odd-ball paradigm in which the CNV was found to peak at the moment of maximum expectation and then to return to baseline for the longer deviant intervals. Furthermore, the CNV became larger and steeper with time-on-task suggesting that this activity could provide an automatic temporal expectancy signal that is being progressively built across the whole experimental session (Mento et al., 2013). At odds with the idea that the late activity following TI-onset indexes the accumulation of pulses over time, we found that the amplitude and the slope of this activity did not significantly vary with RI/TI ratio but instead deflected at 5 s (i.e. the mean of the presented target intervals) for the longer TI-duration. Our results thus suggested that this climbing neuronal activity in the SMA, but also in the PCL and the SFG, reflects an implicit mechanism underlying temporal expectancy based on the temporal context of the experiment (Mento et al., 2013). In keeping with this view, complementary analyses performed for the 7s-TI revealed an effect of the prior TI-duration on two derivations located in the PCL and the SFG. Depending on the derivation, the amplitude of the ICNV-like activity was more important or returned more slowly to baseline when the prior TI-duration was longer (cf figure S5).

4.4. Effects of Emotion on temporal performance and ERPs

Emotional stimuli were used in the encoding phase in order to produce temporal distortions and then to examine correlations with variations in subjective duration induced by emotion. However, behavioral data did not reveal any significant effect of emotion on the *RI/TI ratio*. A possible reason is that the pictures that we selected from the IAPS database were not the most arousing and unpleasant (e.g., pictures of mutilated persons) ones. Their level of arousal

was relatively low compared with that used in previous studies showing a lengthening of perceived duration by the negative emotional charge of pictures (Droit-Volet and Meck, 2007, for review). Concerning SEEG analyses, the emotional effect was modest and was observed for ERPs time-locked to TI-onset in one patient in the anterior insular cortex (AIC), and for ERPs time-locked to TI-offset in another patient in the superior frontal gyrus (SFG). Due to lack of behavioral effect, it is not possible to conclude about a role of these brain regions in emotion-induced distortion of time.

4.5. Limits of the study

Altogether, the results of this intracerebral EEG study revealed that, during reproduction of supra-seconds intervals, the SEEG activity within a network, including primarily the SMA and the insula, is involved just after the ending of the target interval, possibly in the coding of elapsed time during this interval. Interestingly, this activity predicted the trial-to-trial variability in temporal reproduction accuracy. **These results confirm that the monitoring of temporal information continues after the TI-duration and that the neural signatures of interval timing should be explored before and after and not only during the to-be-timed periods (Kononowicz et al., 2017).** However, such interpretations should be considered with cautious due to several limits. First, the filtering characteristics of the SEEG recording system (i.e. time constant = 1.06 sec) could attenuate the low frequencies fluctuations within the raw signal and thus impact the ramping activities during the encoding and the reproduction periods. Further studies should either use longer time constants or investigate shorter durations to determine whether a larger pool of ramping activities associated with interval timing can be observed through SEEG recordings and whether this activity is related to temporal performance. Considering that beta or theta power is assumed to be involved in interval timing (e.g. Bartolo et al., 2014; Gu et al., 2015; Kononowicz and van Rijn, 2015,

2014b; Wiener and Kanai, 2016), an investigation of the dynamics of neural oscillations using SEEG data could help to override the effect of the filter parameters. Further examinations of time-frequency data in SEEG should thus provide valuable information on whether oscillatory power measured during the encoding, the retention and the reproduction periods indexes trial-to-trial variability in temporal reproduction and contribute to determine the neural mechanisms of interval timing.

Second, although several arguments suggest that the observed modulations of ERPs with TI-duration reflect explicit coding of TI-duration, the absence of **non-temporal task** do not allow us to rule out that it actually reflects implicit coding of the TI-duration. It is also not possible to determine whether the observed effects were related to motor preparation or whether similar effects would have been observed in a time discrimination task. In addition, further studies should consider the importance to manipulate the probability of occurrence of the different TI-durations in order to dissociate effects due to elapsed time from effects due to conditional probability. Finally, the results of this SEEG study were obtained in few patients with heterogeneity in electrode location but this limitation is inherent to the SEEG technique. One way to overcome this variability would be to replicate these experiments in a larger sample of patients which altogether will allow a larger coverage of the regions of interest.

5. Conclusions

The aim of the present study was to investigate the dynamics of intracerebral EEG activity into the SMA during the encoding, the retention and the reproduction of time intervals in order to precise their role in interval timing. The results demonstrate that the SEEG activity occurring at the end of the target interval in a network including the SMA as well as frontal, insular and cingulate cortices, varied linearly with TI-duration. This effect indicates that these regions could play a role in the categorization and decision making operations that occur

following the TI-ending or in preparedness and anticipation of the precise moment of the future movement that will be executed to reproduce accurately the target interval. This study, which constitutes the first attempt to examine the neural correlates of time perception by the means of SEEG recordings, also shows the interest of this approach for a better understanding of the neural bases of temporal processing.

Acknowledgements

We thank the patients for willingly accepting to cooperate in this experiment.

Declarations of interest: none

References

- Akkal, D., Escola, L., Bioulac, B., Burbaud, P., 2004. Time predictability modulates pre-supplementary motor area neuronal activity. *Neuroreport* 15 (8), 1283-1286.
- Bartolo, R., Prado, L., Merchant, H., 2014. Information processing in the primate basal ganglia during sensory-guided and internally driven rhythmic tapping. *J. Neurosci.* 34 (11), 3910–3923. doi: 10.1523/JNEUROSCI.2679-13.2014.
- Bendixen, A., Grimm, S., Schröger, E., 2005. Human auditory event-related potentials predict duration judgments. *Neurosci. Lett.* 383 (3), 284-288. doi:10.1016/j.neulet.2005.04.034
- Bueti, D., Macaluso, E., 2011. Physiological correlates of subjective time: evidence for the temporal accumulator hypothesis. *Neuroimage* 57 (3), 1251-1263. doi:10.1016/j.neuroimage.2011.05.014
- Bueti, D., Bahrami, B., Walsh, V., Rees, G., 2010. Encoding of temporal probabilities in the human brain. *J. Neurosci.* 30 (12), 4343-4352. doi: 10.1523/JNEUROSCI.2254-09.2010
- Catani, M., Dell'acqua, F., Vergani, F., Malik, F., Hodge, H., et al., 2012. Short frontal lobe connections of the human brain. *Cortex* 48 (2), 273-291. doi: 10.1016/j.cortex.2011.12.001
- Cauda, F., D'Agata, F., Sacco, K., Duca, S., Geminiani, G., Vercelli, A., 2011. Functional connectivity of the insula in the resting brain. *Neuroimage* 55, 8-23.
- Chiba, A., Oshio, K., Inase, M., 2008. Striatal neurons encoded temporal information in duration discrimination task. *Exp. Brain Res.* 186 (4), 671-676. Doi : 10.1007/s00221-008-1347-3.
- Church, R.M., Meck, W.H., Gibbon, J., 1994. Application of scalar timing theory to individual trials. *J. Exp. Psychol. Anim. Behav. Process.* 20 (2), 135-155.

- Coull, J.T., Vidal, F., Burle, B., 2016. When to act, or not to act: that's the SMA's question. *Curr. Op. Behav. Sci.* 8, 14-21. [10.1016/j.cobeha.2016.01.003](https://doi.org/10.1016/j.cobeha.2016.01.003)
- Coull, J.T., Charras, P., Donadieu, M., Droit-Volet, S., Vidal, F., 2015. SMA Selectively Codes the Active Accumulation of Temporal, Not Spatial, Magnitude. *J. Cogn. Neurosci.* 27 (11), 2281-2298. [doi:10.1162/jocn_a_00854](https://doi.org/10.1162/jocn_a_00854)
- Coull, J.T., 2009. Neural substrates of mounting temporal expectation. *PLoS Biol.* 7, e1000166. [doi: 10.1371/journal.pbio.1000166](https://doi.org/10.1371/journal.pbio.1000166).
- Coull, J.T., Nazarian, B., Vidal, F., 2008. Timing, storage, and comparison of stimulus duration engage discrete anatomical components of a perceptual timing network. *J. Cogn. Neurosci.* 20 (12), 2185-2197. [doi: 10.1162/jocn.2008.20153](https://doi.org/10.1162/jocn.2008.20153).
- Coull, J.T., Vidal, F., Nazarian, B., Macar, F., 2004. Functional anatomy of the attentional modulation of time estimation. *Science* 303 (5663), 1506-1508. [doi:10.1126/science.1091573](https://doi.org/10.1126/science.1091573)
- Cui, X., Stetson, C., Montague, P.R., Eagleman, D.M., 2009. Ready...go: Amplitude of the FMRI signal encodes expectation of cue arrival time. *PLoS Biol* 7, e1000167. [doi:10.1371/journal.pbio.1000167](https://doi.org/10.1371/journal.pbio.1000167)
- Delorme, A., Makeig, S., 2002. EEGLAB: an open source toolbox for analysis of single-trial EEG dynamics including independent component analysis. *J. Neurosci. Methods* 134 (1), 9-21.
- Deen, B., Pitskel, N.B., Pelphrey, K.A., 2011. Three systems of insular functional connectivity identified with cluster analysis. *Cereb. Cortex* 21, 1498-1506.
- Droit-Volet, S., Meck, W.H., 2007. How emotions colour our perception of time. *Trends Cogn. Sci.* 11 (12), 504-513.

- Duysens, J., Schaafsma, S.J., Orban, G.A., 1996. Cortical off response tuning for stimulus duration. *Vision Res.* 36 (20), 3243-3251.
- Elbert, T., Ulrich, R., Rockstroh, B., Lutzenberger, W., 1991. The processing of temporal intervals reflected by CNV-like brain potentials. *Psychophysiology* 28 (6), 648-655.
- Enatsu, R., Gonzalez-Martinez, J., Bulacio, J., Mosher, J.C., Burgess, et al., 2016. Connectivity of the frontal and anterior insular network: a cortico-cortical evoked potential study. *J. Neurosurg.* 125 (1), 90-101. doi: 10.3171/2015.6.JNS15622.
- Genovesio, A., Tsujimoto, S., Wise, S.P., 2009. Feature- and order-based timing representations in the frontal cortex. *Neuron* 63 (2), 254-266. doi:10.1016/j.neuron.2009.06.018
- Gibbon, J., 1977. Scalar expectancy theory and Weber's Law in animal timing. *Psychol. Rev.* 84 (3), 279-325.
- Gibbons, H., Rammsayer, T.H., 2004. Current-source density analysis of slow brain potentials during time estimation. *Psychophysiology* 41 (6), 861-874.
- Gómez, C.M., Marco, J., Grau, C., 2003. Preparatory visuo-motor cortical network of the contingent negative variation estimated by current density. *Neuroimage* 20 (1), 216-224.
- Gontier, E., Paul, I., Le Dantec, C., Pouthas, V., Jean-Marie, G., et al., 2009. ERPs in anterior and posterior regions associated with duration and size discriminations. *Neuropsychology* 23 (5), 668-678.
- Gu, B.-M., van Rijn, H., Meck, W.H., 2015. Oscillatory multiplexing of neural population codes for interval timing and working memory. *Neurosci. Biobehav. Rev.* 48, 160–185. doi: 10.1016/j.neubiorev.2014.10.008.

- Henry, M.J., Herrmann, B., Obleser, J., 2015. Selective attention to temporal features on nested time scales. *Cereb. Cortex* 25 (2), 450-459. doi:10.1093/cercor/bht240
- Herrmann, B., Henry, M.J., Scharinger, M., Obleser, J., 2014. Supplementary motor area activations predict individual differences in temporal-change sensitivity and its illusory distortions. *Neuroimage* 101, 370-379. doi:10.1016/j.neuroimage.2014.07.026
- Ivry, R.B., Spencer, R.M.C., 2004. The neural representation of time. *Curr. Opin. Neurobiol.* 14 (2), 225-232. doi:10.1016/j.conb.2004.03.013
- Jonas, J., Frismand, S., Vignal, J.P., Colnat-Coulbois, S., Koessler, L., et al., 2014. Right hemispheric dominance of visual phenomena evoked by intracerebral stimulation of the human visual cortex. *Hum. Brain Mapp.* 35 (7), 3360-3371. doi: 10.1002/hbm.22407.
- Kononowicz, T., Van Rijn, H., Meck, W., 2017. Timing and Time Perception: A Critical Review of Neural Timing Signatures Before, During, and After the To-Be-Timed Interval. In: Wixted J., Serences J. (Eds), *Stevens' Handbook of Experimental Psychology and Cognitive Neuroscience* (4th ed.), Volume II: Sensation, Perception and Attention, New York: Wiley.
- Kononowicz, T.W., Sander, T., van Rijn, H., 2015. Neuroelectromagnetic signatures of the reproduction of supra-second durations. *Neuropsychologia* 75, 201-213. doi:10.1016/j.neuropsychologia.2015.06.001
- Kononowicz, T.W., van Rijn, H., 2015. Single trial beta oscillations index time estimation. *Neuropsychologia* 75, 381-389. doi:10.1016/j.neuropsychologia.2015.06.014
- Kononowicz, T.W., van Rijn, H., 2014a. Decoupling interval timing and climbing neural activity: a dissociation between CNV and N1P2 amplitudes. *J. Neurosci.* 34 (8), 2931-2939. doi:10.1523/JNEUROSCI.2523-13.2014

- Kononowicz, T. W., van Rijn, H. 2014b. Tonic and phasic dopamine fluctuations as reflected in beta-power predict interval timing behavior. *Procedia Soc Behav Sci*, 126, 47. doi: 10.1016/j.sbspro.2014.02.313
- Kononowicz, T.W., van Rijn, H., 2011. Slow potentials in time estimation: the role of temporal accumulation and habituation. *Front. Integr. Neurosci.* 5 (48).
- Lang, P.J., Bradley, M.M., Cuthbert, B.N., 2008. International affective picture system (IAPS): Affective ratings of pictures and instruction manual. Technical Report A-8. University of Florida. Gainesville, FL.
- Lejeune, H., Wearden, J.H., 2009. Vierordt's the experimental study of the time sense (1868) and its legacy. *Eur. J. Cognit. Psychol.* 21 (6), 941-960. doi.org/10.1080/09541440802453006.
- Lewis, P.A., Miall, R.C., 2003. Brain activation patterns during measurement of sub- and supra-second intervals. *Neuropsychologia* 41 (12), 1583-1592.
- Lindbergh, C.A., Kieffaber, P.D., 2013. The neural correlates of temporal judgments in the duration bisection task. *Neuropsychologia* 51 (2), 191-196.
- Livesey, A.C., Wall, M.B., Smith, A.T., 2007. Time perception: manipulation of task difficulty dissociates clock functions from other cognitive demands. *Neuropsychologia* 45 (2), 321-331. doi:10.1016/j.neuropsychologia.2006.06.033
- Loveless, L., Sanford, S., 1974. Slow potential correlates of preparatory set. *Biol. Psychol.* 1 (4), 303-314.
- Luce, R.D., 1986. *Response times: their role in inferring elementary mental organization.* New York: Oxford University Press.

- Macar, F., Vidal, F., 2003. The CNV peak: An index of decision making and temporal memory. *Psychophysiology* 40 (6), 950-954.
- Macar, F., Vidal, F., 2002. Time processing reflected by EEG surface Laplacians. *Exp. Brain Res.* 145 (3), 403-406. doi:10.1007/s00221-002-1103-z
- Macar, F., Vidal, F., Casini, L., 1999. The supplementary motor area in motor and sensory timing: evidence from slow brain potential changes. *Exp. Brain Res.* 125 (3), 271-280.
- Mayka, M.A., Corcos, D.M., Leurgans, S.E., Vaillancourt, D.E., 2006. Three-dimensional locations and boundaries of motor and premotor cortices as defined by functional brain imaging: a meta-analysis. *Neuroimage* 31 (4), 1453-1474.
- Mendoza G., Méndez J.C., Pérez O, Prado L., Merchant H., 2018. Neural basis for categorical boundaries in the primate pre-SMA during relative categorization of time intervals. *Nat Commun* 19 (1), 1098. doi: 10.1038/s41467-018-03482-8.
- Mento, G., Tarantino, V., Sarlo, M., Bisiacchi, P.S., 2013. Automatic temporal expectancy: a high-density event-related potential study. *PLoS ONE* 8, e62896. doi:10.1371/journal.pone.0062896
- Merchant, H., Harrington, D.L., Meck, W.H., 2013. Neural basis of the perception and estimation of time. *Annu. Rev. Neurosci.* 36, 313-336. doi:10.1146/annurev-neuro-062012-170349
- Mita, A., Mushiake, H., Shima, K., Matsuzaka, Y., Tanji, J., 2009. Interval time coding by neurons in the presupplementary and supplementary motor areas. *Nat. Neurosci.* 12 (4), 502-507. doi: 10.1038/nn.2272.
- Ng, K.K., Yip, P.P.Y., Soh, Y.H., Penney, T.B., 2009. Duration magnitude and memory resource demand. *Neuroquantology* 7 (1), 128-137.

Paul, I., Wearden, J., Bannier, D., Gontier, E., Le Dantec, C., et al., 2011. Making decisions about time: event-related potentials and judgements about the equality of durations. *Biol. Psychol.* 88 (1), 94-103.

Pfeuty, M., Ragot, R., Pouthas, V., 2005. Relationship between CNV and timing of an upcoming event. *Neurosci. Lett.* 382 (1), 106-111.

Pfurtscheller, G., Andrade, A., Koschutnig, K., Brunner, C., Lopes da Silva, F., 2014. Initiation of voluntary movements at free will and ongoing 0.1-Hz BOLD oscillations in the insula - a pilot study. *Front. Integr. Neurosci.* 8, 93. doi: 10.3389/fnint.2014.00093

Pouthas, V., George, N., Poline, J.B., Pfeuty, M., Vandemoortele, P.F., et al., 2005. Neural network involved in time perception: an fMRI study comparing long and short interval estimation. *Hum. Brain Mapp.* 25 (4), 433-441. doi:10.1002/hbm.20126

Sakata, H., Itoh, K., Suzuki, Y., Nakamura, K., Watanabe, M., et al., 2017. Slow Accumulations of Neural Activities in Multiple Cortical Regions Precede Self-Initiation of Movement: An Event-Related fMRI Study. *ENEURO* 4, 5. doi: <http://dx.doi.org/10.1523/ENEURO.0183-17.2017>

Talairach, J., Bancaud, J., 1973. Stereotaxic approach to epilepsy: Methodology of anatomic-functional stereotactic investigations. *Prog. Neurol. Surg.* 5, 297-354.

Tamm, M., Uusberg, A., Allik, J., Kreegipuu, K., 2014. Emotional modulation of attention affects time perception: evidence from event-related potentials. *Acta Psychol.* 149, 148-156.

Tarantino, V., Ehles, A.C., Baehne, C., Boreatti-Huemmer, A., Jacob, C., et al., 2010. The time course of temporal discrimination: an ERP study. *Clin. Neurophysiol.* 121 (1), 43-52.

Taylor, K.S., Seminowicz, D.A., David, K.D., 2009. Two systems of resting state connectivity between insula and cingulate cortex. *Hum. Brain Mapp.* 30, 2731-2745.

- Tipples, J., Brattan, V., Johnston, P., 2013. Neural bases for individual differences in the subjective experience of short durations (less than 2 seconds). *PLoS ONE* 8, e54669. doi:10.1371/journal.pone.0054669
- Tzourio-Mazoyer, N., Landeau, B., Papathanassiou, D., Crivello, F., Etard, O., et al., 2002. Automated anatomical labeling of activations in SPM using a macroscopic anatomical parcellation of the MNI MRI single-subject brain. *Neuroimage* 15 (1), 273-289.
- Vierordt, K. (1868). *Der Zeitsinn nach Versuchen*. Tübingen: Laupp.
- van Rijn, H., Kononowicz, T.W., Meck, W.H., Ng, K.K., Penney, T.B., 2011. Contingent negative variation and its relation to time estimation: a theoretical evaluation. *Front. Integr. Neurosci.* 5, 91. doi:10.3389/fnint.2011.00091
- Wencil, E.B., Coslett, H.B., Aguirre, G.K., Chatterjee, A., 2010. Carving the clock at its component joints: neural bases for interval timing. *J. Neurophysiol.* 104 (1), 160-168. doi:10.1152/jn.00029.2009
- Wiener, M., Kanai, R., 2016. Frequency tuning for temporal perception and prediction. *Curr. Opin. Behav. Sci.* 8, 1–6. doi: 10.1016/j.cobeha.2016.01.001
- Wiener, M., Thompson, J.C., 2015. Repetition enhancement and memory effects for duration. *Neuroimage* 113, 268-278. doi: 10.1016/j.neuroimage.2015.03.054.
- Wiener, M., Thompson, J.C., Coslett, H.B., 2014. Continuous carryover of temporal context dissociates response bias from perceptual influence for duration. *PLoS ONE* 9, e100803. doi: 10.1371/journal.pone.0100803.
- Wiener, M., Turkeltaub, P., Coslett, H.B., 2010. The image of time: a voxel-wise meta-analysis. *Neuroimage* 49 (2), 1728-1740. doi:10.1016/j.neuroimage.2009.09.064

Wittmann, M., Simmons, A.N., Aron, J.L., Paulus, M.P., 2010. Accumulation of neural activity in the posterior insula encodes the passage of time. *Neuropsychologia* 48 (10), 3110-3120. doi:10.1016/j.neuropsychologia.2010.06.023

Table 1. Clinical data and SEEG investigation of the four patients.

Patient	Pat. 1	Pat. 2	Pat. 3	Pat. 4
Age (year)	48	21	20	39
Sex	M	F	M	M
WAIS full scale IQ	75	75	119	85
Epileptogenic zone	Left amygdala, hippocampus, collateral sulcus, temporal pole and lateral pre-motor cortex	Right amygdala, anterior insula and anterior cingulate cortex	Right superior frontal gyrus (supplementary motor area) and mid-cingulate sulcus	Right superior and middle frontal gyrus
Structural lesion	Atrophic lesion in the left temporal polar region	Normal MRI	Normal MRI Right mid-cingulate sulcus focal cortical dysplasia (SEEG investigation)	Normal MRI
Side of focus	L	R	R	R
# of Electrodes L and R	14 L	3 L, 12 R	2 L, 10 R	9 R
# of electrode contacts	160	178	126	113
# of bipolar derivations	107	102	88	93
Structures explored	L: A, ACC, AIC, H, IFG, IPG, ITG, MCC, MFG, MTG, OFC, SFG, SMA, TP	L: ACC, IFG, IPG, MFG, OFC, PCC R: ACC, AIC, H, FP, IFG, ITG, MCC, MFG, MTG, OFC, SFG, SMA, TP	L: SFG, SMA R: ACC, AIC, IFG, MCC, MFG, SFG, SMA	R: ACC, AIC, FP, IFG, MCC, MFG, MO, PIC, PCL, PO, SFG, SMA

Global cognitive efficiency was investigated with the WAIS-III in Pat. 1, the WAIS IV in Pat 2, Pat.3 and Pat. 4.

The structures are listed by subregions in the “Structures Explored” line. A, amygdala; ACC, anterior cingulate cortex; AIC, anterior insular cortex; FP, frontal pole; H, hippocampus; IFG, inferior frontal gyrus; IPG, inferior parietal gyrus; ITG, inferior temporal gyrus; MCC, middle cingulate cortex; MFG, middle frontal gyrus; MO, motor operculum; MTG, middle temporal gyrus; OFC, orbitofrontal cortex; PCC, posterior cingulate cortex; PIC, posterior insular cortex; PCL, paracentral lobule; SFG, superior frontal gyrus; SMA, supplementary motor area; SPG; TP, temporal pole; L, left; R, right.

Table 2. ERPs time-locked to target interval (TI) onset whose amplitude varied (a) with emotion (neutral, negative), or (b) linearly with *RI/TI ratio* (quartiles Q1, Q2, Q3, Q4).

Patient	Region / Brodmann area	Bipolar derivations	Talairach coordinates (x, y, z)	Time windows	t	p value
<i>a. Early ERPs time-locked to TI-onset whose amplitude varied with Emotion</i>						
Pat. 2	R. AIC / BA 13	I2-I3	35, 23, 4	tw2	2.64	.009
<i>b. Early ERPs time-locked to TI-onset whose amplitude varied linearly with RI/TI ratio</i>						
Pat. 3	L. SFG / BA 6	M'9-M'10	-24, 11, 66	tw1	-3.28	.001
	R. IFG / BA 44	O7-O8	57, 4, 16	tw1	-2.34	.021

Time windows of analysis: tw1 = 200-600ms, tw2 = 600-1000ms after TI-onset.
AIC, anterior insular cortex; IFG, inferior frontal gyrus; SFG, superior frontal gyrus.

Table 3. ERPs time-locked to target interval (TI) offset whose amplitude varied linearly with TI-duration (3, 5 and 7 s).

Patient	Region / Brodmann area	Bipolar derivations	Talairach coordinates (x, y, z)	Time windows	t	p value	Bonferroni post-hoc tests					
							3 vs. 5 s	3 vs. 7 s	5 vs. 7 s			
Pat. 2	R. SMA / BA 6	M2-M3	7, -3, 57	tw2	3.77	<.001	.976	.001	.018			
				tw3	2.77	.006	1.000	.019	.030			
				tw4	3.59	<.001	1.000	.001	.002			
				tw5	3.21	.002	1.000	.005	.014			
	R. ACC / BA32	S1-S2	7, 22, 22	tw4	-4.14	<.001	.863	< .001	.008			
				tw5	-3.95	<.001	1.000	< .001	.001			
	R. ACC / BA32	S2-S3	10, 22, 22	tw4	3.27	.001	1.000	.004	< .001			
				tw5	3.80	<.001	1.000	.001	< .001			
	R. MCC / BA 24	R1-R2	6, -1, 32	tw3	-2.95	.004	.067	.011	1.000			
				tw4	-3.52	<.001	.010	.002	1.000			
				tw5	-4.21	<.001	.111	< .001	.109			
				tw6	-3.85	<.001	.210	.001	.130			
	R. MFG / BA 9	S10-S11	38, 26, 27	tw1	-3.22	.002	.109	.005	.810			
				tw2	-2.97	.004	.002	.011	1.000			
				tw4	-3.34	.001	.193	.003	.427			
	R. OFC / BA 10	X10-X11	38, 50, 0	tw4	-3.34	.001	.193	.003	.427			
	R. AIC / BA 13	I1-I2	32, 22, 2	tw3	3.24	.002	.627	.005	.155			
				tw4	3.05	.003	1.000	.009	.125			
				tw5	3.23	.002	1.000	.005	.030			
	R. H / BA 28	B1-B2	22, -11, -21	tw5	3.04	.003	.285	.008	.526			
tw2				2.81	0.006	0.002	0.017	1.000				
R. pSMA / BA 6				M2-M3	8, 7, 56	tw1	5.65	<0.001	0.002	< 0.001	0.078	
R. SMA / BA 6				P1-P2	7, -10, 53	tw4	2.80	0.006	0.134	0.017	1.000	
Pat. 3	R. SMA / BA 6	P1-P2	7, -10, 53	tw5	2.76	0.007	0.089	0.020	1.000			
				tw6	2.86	0.005	0.006	0.014	1.000			
				R. SMA / BA 6	P2-P3	10, -11, 55	tw3	3.08	0.002	0.081	0.007	1.000
				L. pSMA / BA 6	M'2-M'3	-9, 7, 50	tw3	-3.69	<0.001	0.206	0.001	0.204
	L. pSMA / BA 6	M'3-M'4	-11, 8, 52	tw4	-3.40	<0.001	0.669	0.003	0.096			
				tw3	-3.34	0.001	0.094	0.003	0.778			
	R. MCC / BA 24	C2-C3	7, 8, 37	tw2	3.32	0.001	0.020	0.003	1.000			
	R. MCC / BA 32	C3-C4	10, 9, 38	tw1	-4.12	<0.001	0.015	< 0.001	0.660			
				tw4	3.63	<0.001	0.011	0.001	1.000			
	R. SFG / BA 6	M6-M7	19, 9, 64	tw1	-2.84	0.005	0.530	0.016	0.398			
	R. SFG / BA 8	F1-F2	4, 34, 39	tw1	4.55	<0.001	0.032	< 0.001	0.189			
	R. SFG / BA 8	S7-S8	23, 28, 45	tw3	2.91	0.004	0.721	0.013	0.261			
	L. SFG / BA 6	M'6-M'7	-17, 9, 59	tw1	-3.19	0.002	0.465	0.005	0.258			
	L. SFG / BA 6	M'7-M'8	-20, 10, 61	tw2	-3.18	0.002	0.067	0.005	1.000			
	L. SFG / BA 6	M'8-M'9	-22, 10, 64	tw2	3.17	0.002	0.175	0.011	0.846			
	L. SFG / BA 6	M'9-M'10	-24, 11, 66	tw2	2.85	0.006	0.047	0.009	1.000			
	R. MFG / BA 10	X10-X11	35, 43, 20	tw1	-3.10	0.002	1.000	0.007	0.060			
	R. MFG / BA 6	R1-R2	33, -2, 50	tw1	-3.50	<0.001	0.591	0.002	0.087			
	R. MFG / BA 6	R2-R3	36, -2, 50	tw1	-5.16	<0.001	0.090	< 0.001	0.027			
				tw2	-4.78	<0.001	0.038	< 0.001	0.165			
R. MFG / BA 6	R3-R4	40, -2, 50	tw1	5.41	<0.001	0.001	< 0.001	0.338				
			tw2	3.33	0.001	0.012	0.003	1.000				
R. IFG / BA 44	O7-O8	57, 4, 16	tw7	-3.29	0.001	0.002	0.004	1.000				
R. AIC / BA 13	O2-O3	41, 5, 13	tw1	-3.54	<0.001	0.001	0.002	1.000				

Pat. 4	R. pSMA / BA 6	L1-L2	11, 9, 45	tw3	3.14	0.002	0.139	0.006	0.769
				tw4	2.88	0.005	0.034	0.005	1.000
	R. MCC / BA 24	C1-C2	3, -19, 38	tw2	2.78	0.006	0.687	0.018	0.354
	R. SFG / BA 6	X1-X2	6, 22, 49	tw1	2.82	0.005	1.000	0.016	0.182
				tw2	4.53	<0.001	0.390	<0.001	0.010
				tw3	4.51	<0.001	0.521	<0.001	0.006
				tw4	4.72	<0.001	0.221	<0.001	0.013
				tw5	4.69	<0.001	0.101	<0.001	0.036
				tw6	4.32	<0.001	0.101	<0.001	0.094
				tw7	4.21	<0.001	0.049	<0.001	0.229
	R. SFG / BA 6	X5-X6	11, 23, 62	tw2	-3.27	0.001	0.446	0.004	0.224
				tw3	-3.71	<0.001	0.006	0.001	1.000
				tw4	-3.04	0.003	0.018	0.009	1.000
				tw6	-2.91	0.004	0.260	0.013	0.729
	R. MFG / BA 8	F9-F10	32, 22, 39	tw5	2.99	0.003	1.000	0.010	0.052
				tw7	3.49	<0.001	1.000	0.002	0.014
	R. IFG / BA 44	B1-B2	31, 16, 24	tw1	3.58	<0.001	0.989	0.001	0.033
				tw2	3.62	<0.001	0.587	0.001	0.070
	R. PCL / BA 6	M2-M3	6, -16, 54	tw3	-3.78	<0.001	0.055	0.001	0.498
				tw4	-3.38	<0.001	0.093	0.003	0.690
				tw5	-3.59	<0.001	0.010	0.001	1.000
				tw6	-3.37	<0.001	0.007	0.003	1.000
				tw7	-3.91	<0.001	0.002	<0.001	1.000
	R. PCL / BA 6	M6-M7	15, -16, 66	tw1	3.52	<0.001	0.341	0.003	0.219
				tw2	2.90	0.004	0.559	0.013	0.366
	R. PCL / BA 6	M7-M8	17, -16, 69	tw3	3.47	<0.001	1.000	0.002	0.001
				tw4	3.90	<0.001	1.000	<0.001	0.004
				tw6	3.62	<0.001	0.759	0.001	0.048
				tw7	3.61	<0.001	0.221	<0.001	0.114
	R. PCL / BA 6	M8-M9	19, -16, 72	tw1	-3.04	0.004	0.771	0.012	0.227
	R. PCL / BA 6	P4-P5	14, -29, 57	tw3	-2.80	0.006	0.348	0.018	0.679
				tw4	-4.33	<0.001	0.324	<0.001	0.022
				tw5	-3.94	<0.001	0.570	<0.001	0.029
				tw6	-3.78	<0.001	0.108	0.001	0.298
				tw7	-4.30	<0.001	0.012	<0.001	0.523
	R. PIC / BA 13	R3-R4	45, -30, 18	tw4	3.48	<0.001	0.027	0.002	1.000
	R. PIC / BA 13	R6-R7	54, -34, 19	tw1	-3.89	<0.001	0.138	0.001	0.150
				tw2	-3.60	<0.001	0.148	0.002	0.269

Time Windows of analysis: tw1 = 200-600ms, tw2 = 600-1000ms, tw3 = 1000-1400ms, tw4 = 1400-1800ms, tw5 = 1800-2200ms, tw6 = 2200-2600ms, tw7 = 2600-3000ms after TI-offset.

AIC, anterior insular cortex; ACC, anterior cingulate cortex; H, Hippocampus; IFG, inferior frontal gyrus; MCC, middle cingulate cortex; MFG, middle frontal gyrus; OFC, orbitofrontal cortex; PCL, paracentral lobule; PIC, posterior insular cortex; pSMA, pre-supplementary motor area; SFG, superior frontal gyrus; SMA, supplementary motor area proper. Significant Bonferroni post-hoc p values are noted in bold.

Table 4. Brain regions in which the amplitude of ERPs time-locked to target interval (TI) offset varied linearly with TI-duration (3, 5, 7s). Number of electrodes contacts (within each brain region) showing an effect of TI-duration over the successive time-windows (tw1 to tw7).

Regions	tw1	tw2	tw3	tw4	tw5	tw6	tw7
SMA/pSMA	2	4	9	8	4	2	0
SFG	8	8	6	4	2	4	1
MFG	8	5	0	0	2	0	2
IFG	2	2	0	0	0	0	2
OFC	0	0	0	2	0	0	0
PCL	4	2	6	6	5	6	6
ACC/MCC	2	4	2	7	5	2	2
IC	4	2	2	4	2	0	0
Extra-frontal	0	0	0	0	2	0	0
-----	-----	-----	-----	-----	-----	-----	-----
TOTAL	30	27	25	31	22	14	13

Time Windows of analysis: tw1 = 200-600 ms, tw2 = 600-1000 ms,
tw3 = 1000-1400 ms, tw4 = 1400-1800 ms, tw5 = 1800-2200 ms,
tw6 = 2200-2600 ms, tw7 = 2600-3000 ms after TI-offset.

IC, insular cortex; IFG, inferior frontal gyrus;

MCC/ACC, middle and anterior cingulate cortex; MFG, middle frontal gyrus;

OFC, orbitofrontal cortex; PCL, paracentral lobule; SFG, superior frontal gyrus;

SMA/pSMA, supplementary and pre-supplementary motor areas.

Table 5. ERPs time-locked to target interval (TI) offset whose amplitude varied (a) with emotion (neutral, negative), or (b) linearly with *RI/TI ratio* (quartiles Q1, Q2, Q3, Q4).

Patient	Region / Brodmann area	Bipolar derivations	Talairach coordinates (x, y, z)	Time windows	t	p value
<i>a. Early ERPs time-locked to TI-offset whose amplitude varied with Emotion</i>						
Pat. 3	R. SFG / BA 9	G3-G4	12, 34, 34	tw2	3.15	.002
				tw5	3.65	<.001
				tw6	3.46	<.001
				tw7	3.46	<.001
<i>b. Early ERPs time-locked to TI-offset whose amplitude varied linearly with RI/TI ratio</i>						
Pat. 4	R. MCC / BA 24	C1-C2	3, -19, 38	tw1	-3.28	.001

Time windows of analysis: tw1 = 200-600ms, tw2 = 600-1000ms after TI-offset.
MCC, middle cingulate cortex; SFG, superior frontal gyrus.

Table 6. ERPs time-locked to reproduction interval (*RI*) onset whose amplitude varied linearly with target interval (*TI*) duration (3, 5 and 7 s).

Patient	Region / brodmann area	Bipolar derivations	Talairach coordinates (x, y, z)	Time windows	t	p value	Bonferroni post-hoc tests		
							3 vs. 5 s	3 vs. 7 s	5 vs. 7 s
Pat. 3	R. MFG / BA 6	R2-R3	36, -2, 50	tw2	2.71	.008	.897	.023	.272
	R. MFG / BA 6	R3-R4	40, -2, 50	tw2	-2.53	.013	1.00	.038	.179
Pat. 4	R. MFG / BA 46	G11-G12	42, 41, 26	tw1	2.71	.008	.319	.023	.870
	R. PCL / BA 2	P11-P12	38, -35, 57	tw1	2.82	.006	.337	.017	.680

Time Windows of analysis: tw1 = 200-600ms, tw2 = 600-1000ms after RI-onset.

MFG, middle frontal gyrus; PCL, paracentral lobule.

Significant Bonferroni post-hoc p values are noted in bold.

Table 7. ERPs time-locked to reproduction interval (*RI*) onset whose amplitude varied linearly with *RI/ITI ratio* (quartiles Q1, Q2, Q3, Q4).

Patient	Region / Brodmann area	Bipolar derivations	Talairach coordinates (x, y, z)	Time windows	t	p value
Pat. 3	R. MFG / BA 8	C7-C8	22, 13, 43	tw1	3.24	.002
				tw2	2.68	.008
	R. MCC / BA 32	C6-C7	19, 12, 42	tw1	-3.39	.001
				tw2	-2.30	.023
Pat. 4	R. pSMA / BA 6	L1-L2	11, 9, 45	tw1	-2.74	.007
				tw2	-2.51	.013
	R. IFG / BA 44	B1-B2	31, 16, 24	tw1	2.58	.011
				tw2	4.68	<.001

Time Windows of analysis: tw1 = 200-600ms, tw2 = 600-1000 ms after RI-onset.
 IFG, inferior frontal gyrus; MCC, middle cingulate cortex; MFG, middle frontal gyrus;
 pSMA, pre-supplementary motor area.

Table S1. Behavioral data and statistical analyses.

Patient		Pat. 1			Pat. 2			Pat. 3			Pat. 4		
a. Mean <i>RI</i>, <i>RI/TI</i> ratio and <i>CV</i> measured for each <i>TI</i>-duration (3, 5 and 7 s) and emotion (Nt and Ng) in each patient													
		<i>RI</i> (ms)	<i>RI/TI</i> ratio	<i>CV</i>	<i>RI</i> (ms)	<i>RI/TI</i> ratio	<i>CV</i>	<i>RI</i> (ms)	<i>RI/TI</i> ratio	<i>CV</i>	<i>RI</i> (ms)	<i>RI/TI</i> ratio	<i>CV</i>
3 s	Nt	3250	1.08	0.46	3730	1.24	0.30	2798	0.93	0.14	3681	1.23	0.17
	Ng	3389	1.13	0.34	3565	1.19	0.30	2741	0.91	0.19	4166	1.39	0.19
5 s	Nt	3352	0.67	0.28	5523	1.10	0.22	4954	0.99	0.11	5091	1.02	0.18
	Ng	3979	0.80	0.38	6022	1.20	0.19	4747	0.95	0.13	5252	1.05	0.24
7 s	Nt	4034	0.58	0.32	7330	1.05	0.18	6638	0.95	0.07	6565	0.94	0.21
	Ng	3552	0.51	0.25	7363	1.05	0.26	6445	0.92	0.10	6442	0.92	0.16
b. Effect of <i>TI</i>-duration on the <i>RI</i>													
One-way ANOVA	t	1.89			13.88			34.43			12.80		
	df	144			146			147			147		
	p value	.061			<.001			<.001			<.001		
Cohen's d [95% CI]	3 vs. 5 s	0.26 [-0.14, 0.66]			1.84 [1.37, 2.31]			3.90 [3.23, 4.56]			1.32 [0.89, 1.76]		
	3 vs. 7 s	0.39 [-0.01, 0.79]			2.69 [2.14, 3.23]			7.22 [6.14, 8.29]			2.56 [2.03, 3.09]		
	5 vs. 7 s	0.11 [-0.28, 0.51]			1.10 [0.68, 1.52]			2.89 [2.32, 3.45]			1.15 [0.73, 1.58]		
c. Effect of <i>TI</i>-duration and Emotion on the <i>RI/TI</i> ratio													
Effect of <i>TI</i> -duration	F	43.61			4.33			2.00			41.84		
	df	2, 141			2, 143			2, 144			2, 144		
	p value	<.001			.015			.139			<.001		
Bonferroni post-hoc tests	3 vs. 5 s	<.001			.851			.175			<.001		
	3 vs. 7 s	<.001			.012			1.00			<.001		
	5 vs. 7 s	.007			.199			.425			.047		
Effect of Emotion	F	0.48			0.13			2.07			2.80		
	df	1, 141			1, 143			1, 144			1, 144		
	p value	.490			.722			.152			.096		
<i>TI</i> -duration × Emotion	F	1.29			0.93			0.10			2.31		
	df	2, 141			2, 143			2, 144			2, 144		
	P value	.278			.397			.903			.103		

TI: Target Interval; *RI*: Reproduction Interval; *CV*: Coefficient of Variation = Standard Deviation of *RI* / Mean of *RI*; *RI/TI* ratio: ratio between the reproduction interval and the *TI*-duration; Nt: emotionally neutral stimuli; Ng: emotionally negative stimuli. Significant p values are noted in bold.

Table S2. ERPs time-locked to TI offset whose amplitude varied linearly with TI-duration (3, 5 and 7 s). Effects of TI-duration over the first (P1) and second (P2) parts of the experiment.

Patient	Region / Brodmann area	Bipolar derivations	Talairach coordinates (x, y, z)	Time windows	First part (P1)		Second part (P2)	
					t	p value	t	p value
Pat. 2	R. SMA / BA 6	M2-M3	7, -3, 57	tw2	-3.44	.001	-2.04	.035
				tw3	-1.65	.104	-2.21	.031
				tw4	-2.15	.035	-2.88	.005
				tw5	-2.33	.023	-2.18	.032
	R.ACC / BA 32	S1-S2	7, 22, 22	tw4	2.69	.009	3.12	.003
				tw5	2.46	.016	3.06	.003
	R.ACC / BA 32	S2-S3	10, 22, 22	tw4	-3.02	.004	-1.62	.110
				tw5	-3.26	.002	-2.08	.043
	R. MCC / BA 24	R1-R2	6, -1, 32	tw3	1.20	.132	2.98	.004
				tw4	2.14	.035	2.80	.007
				tw5	2.25	.027	3.61	.001
				tw6	1.90	.061	3.43	.001
	R. MFG / BA 9	S10-S11	38, 26, 27	tw1	2.66	.010	1.89	.063
				tw2	1.92	.059	2.29	.025
				tw4	2.14	.036	2.59	.012
	R. OFC / BA 10	X10-X11	38, 5, 0	tw4	2.14	.036	2.59	.012
	R. AIC / BA 13	I1-I2	32, 22, 2	tw3	-2.72	.010	-2.34	.024
				tw4	-2.29	.031	-2.19	.034
				tw5	-3.80	.001	-0.95	.349
	R. H / BA 28	B1-B2	22, -11, -21	tw5	-2.31	.024	-1.97	.053
Pat. 3	R. pSMA / BA 6	M1-M2	5, 6, 54	tw2	-1.53	.130	-2.41	.019
	R. pSMA / BA 6	M2-M3	8, 7, 56	tw1	-3.70	<.001	-4.25	<.001
	R. SMA / BA 6	P1-P2	7, -10, 53	tw4	-1.35	.182	-2.56	.012
				tw5	-1.10	.276	-2.76	.007
				tw6	-0.62	.536	-3.46	.001
				tw3	-0.90	.373	-3.78	<.001
	R. SMA / BA 6	P2-P3	10, -11, 55	tw3	-0.90	.373	-3.78	<.001
	L. pSMA / BA 6	M'2-M'3	-9, 7, 50	tw3	1.61	.114	3.85	<.001
				tw4	1.30	.197	3.49	.001
	L. pSMA / BA 6	M'3-M'4	-11, 8, 52	tw3	2.38	.023	2.49	.015
	R. MCC / BA 24	C2-C3	7, 8, 37	tw2	-2.86	.006	-1.87	.066
	R. MCC / BA 32	C3-C4	10, 9, 38	tw1	5.10	<.001	1.00	.322
				tw4	-1.17	.224	-3.81	<.001
	R. SFG / BA 6	M6-M7	19, 9, 64	tw1	2.27	.026	1.80	.076
	R. SFG / BA 8	F1-F2	4, 34, 39	tw1	-2.12	.039	-4.31	<.001
	R. SFG / BA 8	S7-S8	23, 28, 45	tw3	-1.62	.109	-2.42	.018
	L. SFG / BA 6	M'6-M'7	-17, 9, 59	tw1	1.21	.230	3.23	.002
	L. SFG / BA 6	M'7-M'8	-20, 10, 61	tw2	2.06	.043	2.49	.015
	L. SFG / BA 6	M'8-M'9	-22, 10, 64	tw2	-1.67	.099	-2.82	.009
	L. SFG / BA 6	M'9-M'10	-24, 11, 66	tw2	-1.31	.195	-2.71	.011
	R. MFG / BA 10	X10-X11	35, 43, 20	tw1	3.68	<.001	0.92	.360
	R. MFG / BA 6	R1-R2	33, -2, 50	tw1	2.28	.025	2.66	.010
	R. MFG / BA 6	R2-R3	36, -2, 50	tw1	4.83	<.001	2.72	.009
				tw2	4.06	<.001	2.72	.009
	R. MFG / BA 6	R3-R4	40, -2, 50	tw1	-4.32	<.001	-3.27	.002
				tw2	-2.27	.026	-2.43	.018
R. IFG / BA 44	O7-O8	57, 4, 16	tw7	2.19	.032	2.47	.016	
R. AIC / BA 13	O2-O3	41, 5, 13	tw1	3.09	.003	1.96	.054	

Pat. 4	R. pSMA / BA 6	L1-L2	11, 9, 45	tw3	-1.07	.287	-3.17	.003			
				tw4	1.34	.189	-3.00	.004			
	R. MCC / BA 24	C1-C2	3, -20, 38	tw2	-3.29	.002	-0.68	.501			
	R. SFG / BA 6	X1-X2	6, 22, 49	tw1	-1.19	.239	-2.65	.010			
				tw2	-3.04	.003	-3.31	.001			
				tw3	-3.24	.002	-3.10	.003			
				tw4	-3.39	.001	-3.26	.002			
				tw5	-3.36	.001	-3.23	.002			
				tw6	-3.16	.002	-2.92	.005			
				tw7	-3.12	.003	-2.82	.006			
	R. SFG/ BA 6	X5-X6	11, 23, 62	tw2	2.96	.004	1.54	.128			
				tw3	3.25	.002	1.92	.060			
				tw4	1.99	.050	2.30	.025			
				tw6	2.09	.040	2.03	.047			
	R. MFG/ BA8	F9-F10	32, 22, 39	tw5	-3.30	.002	-1.02	.312			
				tw7	-2.34	.023	-2.56	.020			
	R. IFG / BA 44	B1-B2	31, 16, 24	tw1	-2.78	.007	-2.33	.023			
				tw2	-3.80	<.001	-1.57	.120			
	R. PCL / BA6	M2-M3	6, -16, 54	tw3	3.81	<.001	1.65	.102			
				tw4	3.08	.003	1.79	.078			
				tw5	2.73	.008	2.40	.019			
				tw6	2.94	.004	1.83	.071			
				tw7	3.15	.002	2.42	.018			
				R. PCL / BA 6	M6-M7	15, -16, 66	tw1	-1.41	.163	-3.51	.001
							tw2	-0.76	.449	-3.22	.002
	R. PCL / BA 6	M7-M8	17, -16, 69	tw3	-2.11	.039	-2.72	.008			
				tw4	-3.33	.001	-2.42	.019			
				tw6	-2.39	.020	-2.66	.010			
				tw7	-2.98	.004	-2.51	.015			
				tw1	1.56	.167	2.98	.007			
	R. PCL / BA 6	P4-P5	14, -29, 57	tw3	1.98	.052	1.97	.052			
				tw4	3.25	.002	2.86	.006			
				tw5	2.58	.012	2.93	.005			
				tw6	2.54	.013	2.81	.006			
				tw7	2.63	.010	3.47	.001			
	R. PIC / BA 13	R3-R4	45, -30, 18	tw4	-3.26	.002	-1.95	.055			
				tw1	2.62	.012	2.93	.005			
	R. PIC / BA 13	R6-R7	54, -34, 19	tw2	3.51	.001	1.93	.060			

Time Windows of analysis: tw1 = 200-600ms, tw2 = 600-1000ms, tw3 = 1000-1400ms, tw4 = 1400-1800ms, tw5 = 1800-2200ms, tw6 = 2200-2600ms, tw7 = 2600-3000ms after TI-offset. Significant p values are noted in bold. See Table 3 for abbreviations.

Table S3. Post-Target Interval activity indexes predicted by (a) the TI-duration presented in the current trial, and (b) the TI-duration presented in the prior trial (controlling for the effect of the TI-duration presented in the current trial).

Patient	Region / Brodmann area	Bipolar derivations	Talairach coordinates (x, y, z)	Activity index	(a)			(b)		
					β	t	p value	β	t	p value
Pat. 2	R. SMA / BA 6	M2-M3	7, -3, 57	T2-5	0.31	3.93	<.001			
	R. ACC / BA24	S1-S2	7, 22, 22	T4-5	-0.33	-4.25	<.001			
	R. ACC / BA24	S2-S3	1, 22, 22	T4-5	0.22	2.68	.008			
	R. MCC / BA 24	R1-R2	6, -1, 32	T3-7	-0.37	-4.80	<.001	-0.16	-1.98	.049
	R. MFG / BA 9	S10-S11	38, 26, 27	T1-2	-0.26	-3.34	.001			
	R. OFC / BA 10	X10-X11	38, 50, 0	T4	-0.27	-3.35	.001	0.18	2.15	.033
	R. AIC / BA 13	I1-I2	32, 22, 2	T3-5	0.35	3.71	<.001			
	R. H / BA 28	B1-B2	20, -6, -24	T5	0.26	3.06	.003			
Pat. 3	R. pSMA / BA 6	M1-M2	5, 6, 54	P12	-0.39	-4.91	<.001			
	R. pSMA / BA 6	M2-M3	8, 7, 56	P31	-0.55	-7.59	<.001			
	R. SMA / BA 6	P1-P2	7, -10, 53	T46	0.26	3.14	.002			
	R. SMA / BA 6	P2-P3	10, -11, 55	P13	-0.30	-3.64	<.001			
	L. pSMA/ BA 6	M'2-M'3	-9, 7, 50	T34	-0.30	-3.75	<.001	0.19	2.35	.020
	L. pSMA/ BA 6	M'3-M'4	-11, 8, 52	P31	-0.36	-4.53	<.001			
	R. MCC / BA 24	C2-C3	7, 8, 37	P42	-0.39	-4.87	<.001			
	R. MCC / BA 32	C3-C4	10, 9, 38	P14	-0.57	-7.87	<.001	0.24	3.32	.001
	R. SFG / BA 6	M6-M7	19, 9, 64	P13	-0.24	-2.81	.006			
	R. SFG / BA 8	F1-F2	4, 34, 39	P21	-0.41	-4.95	<.001	0.19	2.29	.024
	L. SFG / BA 6	M'6-M'7	-17, 9, 59	P15	-0.23	-2.72	.006			
	L. SFG / BA 6	M'7-M'8	-20, 10, 61	P24	-0.23	-2.70	.008			
	L. SFG / BA 6	M'8-M'9	-22, 10, 64	P42	-0.26	-2.81	.006			
	L. SFG / BA 6	M'9-M'10	-24, 11, 66	P42	-0.28	-2.98	.004	0.38	4.22	<.001
	R. SFG / BA 8	S7-S8	23, 28, 45	P13	-0.17	-2.07	.040			
	R. MFG / BA 10	X10-X11	35, 43, 20	P13	-0.20	-2.44	.016			
	R. MFG / BA 6	R1-R2	33, -2, 50	P12	-0.46	-6.12	<.001	0.26	3.44	.001
	R. MFG / BA 6	R2-R3	36, -2, 50	P14	-0.42	-4.51	<.001			
	R. MFG / BA 6	R3-R4	40, -2, 50	P31	-0.44	-5.66	<.001			
	R. IFG / BA 6	O7-O8	57, 4, 16	T7	-0.26	-3.14	.002	0.18	2.20	.030
R. AIC / BA 13	O2-O3	41, 5, 13	P15	-0.40	-5.10	<.001				
Pat. 4	R. pSMA / BA 6	L1-L2	11, 9, 45	T3-4	0.28	3.32	.001			
	R. MCC / BA 24	C1-C2	3, -20, 38	P4-2	-0.23	-2.81	.006			
	R. SFG / BA 6	X1-X2	6, 22, 49	T1-7	0.37	4.60	<.001			
	R. SFG / BA 6	X5-X6	11, 23, 62	T2-6	-0.32	-3.70	<.001			
	R. MFG / BA 8	F9-F10	32, 22, 39	P3-7	-0.30	-3.50	<.001			
	R. IFG / BA 44	B1-B2	31, 16, 24	P6-2	-0.29	-3.55	<.001			
	R. PCL / BA 6	M2-M3	6, -16, 54	T3-7	-0.31	-3.79	<.001			
	R. PCL / BA 6	M6-M7	15, -16, 66	P3-1	-0.24	-2.72	.008	0.18	2.00	.048
	R. PCL / BA 6	M7-M8	17, -16, 69	T3-7	0.35	4.06	<.001			
	R. PCL / BA 6	M8-M9	19, -16, 72	P1-3	-0.23	-2.28	.025			
	R. PCL / BA 6	P4-P5	14, -29, 57	T3-7	-0.35	-4.30	<.001			
	R. PIC / BA 13	R3-R4	45, -30, 18	T4	0.27	3.35	.001			
	R. PIC / BA 13	R6-R7	54, -34, 19	P1-4	-0.26	-2.58	.012			

P or T: phasic or tonic post-interval activity index. For example, P2-5 corresponds to the amplitude measured on the second time window minus that measured on the fifth time window, whereas T2-5 corresponds to the mean of the amplitudes

measured from the second to the fifth time window. Only significant results are presented in the second series of regression analyses (b). See Table 3 for abbreviations.

Table S4. Post-Target Interval activity indexes (a) predicting the reproduction interval (RI), and (b) predicting the *RI/TI ratio* (controlling for the effect of TI-duration in patients 2 and 4).

Patient	Region / Brodmann area	Bipolar derivations	Talairach coordinates (x, y, z)	Activity index	(a)			(b)		
					β	t	p value	β	t	p value
Pat. 2	R. SMA / BA 6	M2-M3	7, -3, 57	T2-5	0.34	4.34	<.001	0.21	2.58	.011
	R. ACC / BA24	S1-S2	7, 22, 22	T4-5	-0.17	-2.11	.037			
	R. ACC / BA24	S2-S3	1, 22, 22	T4-5	0.09	1.09	.279			
	R. MCC / BA 24	R1-R2	6, -1, 32	T3-7	-0.17	-2.15	.033			
	R. MFG / BA 9	S10-S11	38, 26, 27	T1-2	-0.21	2.63	.009			
	R. OFC / BA 10	X10-X11	38, 50, 0	T4	-0.20	-2.51	.013			
	R. AIC / BA 13	I1-I2	32, 22, 2	T3-5	0.22	2.25	.026			
	R. H / BA 28	B1-B2	20, -6, -24	T5	0.14	1.67	.098			
Pat. 3	R. pSMA / BA 6	M1-M2	5, 6, 54	P1-2	-0.42	-5.50	<.001	-0.16	-2.01	.047
	R. pSMA / BA 6	M2-M3	8, 7, 56	P3-1	-0.53	-7.48	<.001			
	R. SMA / BA 6	P1-P2	7, -10, 53	T4-6	0.26	3.23	.002			
	R. SMA / BA 6	P2-P3	10, -11, 55	P1-3	-0.33	-4.19	<.001			
	L. pSMA / BA 6	M'2-M'3	-9, 7, 50	T3-4	-0.29	-3.72	<.001			
	L. pSMA / BA 6	M'3-M'4	-11, 8, 52	P3-1	-0.34	-4.39	<.001			
	R. MCC / BA 24	C2-C3	7, 8, 37	P4-2	-0.39	-5.06	<.001			
	R. MCC / BA 32	C3-C4	10, 9, 38	P1-4	-0.59	-8.58	<.001			
	R. SFG / BA 6	M6-M7	19, 9, 64	P1-3	-0.25	-3.07	.003			
	R. SFG / BA 8	F1-F2	4, 34, 39	P2-1	-0.42	-5.31	<.001			
	L. SFG / BA 6	M'6-M'7	-17, 9, 59	P1-5	-0.20	-2.43	.016			
	L. SFG / BA 6	M'7-M'8	-20, 10, 61	P2-4	-0.22	-2.72	.007			
	L. SFG / BA 6	M'8-M'9	-22, 10, 64	P4-2	-0.26	-2.96	.004			
	L. SFG / BA 6	M'9-M'10	-24, 11, 66	P4-2	-0.28	-3.10	.002			
	R. SFG / BA 8	S7-S8	23, 28, 45	P1-3	-0.13	-1.59	.114			
	R. MFG / BA 10	X10-X11	35, 43, 20	P1-5	-0.22	-2.74	.007			
	R. MFG / BA 6	R1-R2	33, -2, 50	P1-2	-0.43	-5.75	<.001			
	R. MFG / BA 6	R2-R3	36, -2, 50	P1-4	-0.37	-4.04	<.001			
	R. MFG / BA 6	R3-R4	40, -2, 50	P3-1	-0.42	-5.50	<.001			
	R. PCL / BA 6	O7-O8	57, 4, 16	T7	-0.27	-3.36	.001			
R. AIC / BA 13	O2-O3	41, 5, 13	P1-5	-0.40	-5.26	<.001				
Pat. 4	R. pSMA / BA 6	L1-L2	11, 9, 45	T3-4	0.21	2.51	.013	-0.26	-3.64	<.001
	R. MCC / BA 24	C1-C2	3, -20, 38	P4-2	0.16	2.01	.046			
	R. SFG / BA 6	X1-X2	6, 22, 49	T1-7	0.27	3.33	.001			
	R. SFG / BA 6	X5-X6	11, 23, 62	T2-6	-0.19	-2.20	.030			
	R. MFG / BA 8	F9-F10	32, 22, 39	P3-7	-0.19	-2.20	.021			
	R. IFG / BA 44	B1-B2	31, 16, 24	P6-2	-0.29	-3.68	<.001			
	R. PCL / BA 6	M2-M3	6, -16, 54	T3-7	-0.19	-2.37	.019			
	R. PCL / BA 6	M6-M7	15, -16, 66	P3-1	-0.35	-4.21	<.001			
	R. PCL / BA 6	M7-M8	17, -16, 69	T3-7	0.19	2.20	.029			
	R. PCL / BA 6	M8-M9	19, -16, 72	P1-3	-0.43	-4.90	<.001			
	R. PCL / BA 6	P4-P5	14, -29, 57	T3-7	-0.22	-2.78	.006			
	R. PIC / BA 13	R3-R4	45, -30, 18	T4	0.08	0.99	.322			
	R. PIC / BA 13	R6-R7	54, -34, 19	P1-4	-0.32	-3.30	.001			

P or T: phasic or tonic post-interval activity index. For example, P2-5 corresponds to the amplitude measured on the second time window minus that measured on the fifth time window, whereas T2-5 corresponds to the mean of the amplitudes measured from the second to the fifth time window. Only significant results are presented in the second series of regression analyses (b). See Table 3 for abbreviations.

Figure 1. Schematic representation of the reproduction task. A neutral or emotional picture was presented during the target interval whereas a grey square was presented during the reproduction interval.

Figure 2. The reproduction time (a) and the *RI/TI ratio* (b) measured for the 3, 5 and 7 s-TI in the four patients (*: <0.05; ***: <0.001, after Bonferroni correction). Horizontal dashed lines in figure 2a indicate the TI-duration (deep grey: 7s; grey: 5s; light grey: 3 s). TI: Target Interval; RI: Reproduction Interval.

Figure 3. Proportion of trials per reproduction time for each target interval duration (TI = 3, 5 and 7 s) in each patient. Vertical dashed lines indicate the TI-duration (deep grey: 7s; grey: 5s; light grey: 3 s).

Figure 4. ERP recorded in the supplementary motor area (SMA), the superior frontal gyrus (SFG) and the paracentral lobule (PCL) time-locked to target interval (TI) onset and whose slope calculated between 3 and 5s was different from zero and in the same direction as slope between 1 and 3s for the 5s-TI and the 7s-TI and whose slope between 5 and 7s was not significant different from zero for the 7s-TI (deep grey: 7s; grey: 5s; light grey: 3 s).

Figure 5. ERPs recorded in the supplementary and pre-supplementary motor areas (SMA/pSMA) time-locked to target interval (TI) offset and whose amplitude varied linearly with TI-duration (deep grey: 7s; grey: 5s; light grey: 3 s), except for patient 1. The arrows indicate the time windows for which the ERPs significantly decreased in amplitude with TI-duration. ERP waveforms are temporally smoothed using sliding time windows of 100-ms width. See Table 3 for abbreviations.

Figure 6. ERPs recorded outside of the SMA/pSMA time-locked to target interval (TI) offset and whose amplitude varied linearly with TI-duration (deep grey: 7s; grey: 5s; light grey: 3 s). The arrows indicate the time windows for which the ERPs significantly decreased in amplitude with TI-duration. ERP waveforms are temporally smoothed using sliding time-windows of 100-ms width. See Table 3 for abbreviations.

Figure 7. Spatial distribution of electrode contacts on a schematic brain representation (Talairach and Tournoux coordinates). Cross, square, triangle and circle symbols correspond to contacts in patients 1, 2, 3 and 4, respectively. The sites where the amplitude of ERPs time-locked to target interval (TI) offset varied linearly with TI-duration (3, 5 and 7 s) are noted in large and filled symbols. The transparent grey squares delineate the boundaries of the supplementary and pre-supplementary motor areas (SMA/pSMA) corresponding to the most restricted boundaries of the mesial premotor cortex reported by Mayka et al. (2006). Abbreviations: VAC, vertical line through the anterior commissure; VPC, vertical line through the posterior commissure.

Figure 8. Number of patients and ratios of electrode contacts showing a modulation of ERPs time-locked to target interval (TI) offset with TI-duration by brain region. See Table 3 for abbreviations.

Figure S1. ERPs time-locked to target interval (TI) onset whose amplitude (a) varied according to emotion (neutral: grey line, negative: black line) and (b) varied linearly with *RI/TI ratio* (quartiles are in shades of grey, from the lightest to the darkest: Q1, Q2, Q3 & Q4). The arrows indicate the time windows for which the amplitude of ERPs varied

significantly with emotion (a) and with *RI/TI ratio* (b). ERP waveforms are temporally smoothed using sliding time windows of 100-ms width. See Table 3 for abbreviations.

Figure S2. ERPs time-locked to target interval (TI) offset whose amplitude (a) varied according to emotion (neutral: grey line, negative: black line) and (b) varied linearly with *RI/TI ratio* (quartiles are in shades of grey, from the lightest to the darkest: Q1, Q2, Q3 & Q4). The arrows indicate the time windows for which the amplitude of ERPs varied significantly with emotion (a) and with *RI/TI ratio* (b). ERP waveforms are temporally smoothed using sliding time windows of 100-ms width. See Table 3 for abbreviations.

Figure S3. ERPs time-locked to reproduction interval (RI) onset whose amplitude varied linearly (a) with TI-duration (deep grey: 7s; grey: 5s; light grey: 3 s) and (b) with *RI/TI ratio* (quartiles are in shades of grey, from the lightest to the darkest: Q1, Q2, Q3 & Q4). The arrows indicate the time windows for which the amplitude of ERPs varied significantly with TI-duration (a) and with *RI/TI ratio* (b). ERP waveforms are temporally smoothed using sliding time windows of 100-ms width. See Table 3 for abbreviations.

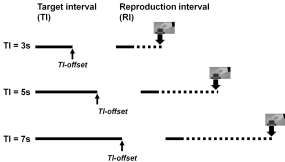
Figure S4. Ratios of electrode contacts showing a modulation of ERPs time-locked to target interval (TI) offset with TI-duration by brain region and for each part of the experiment (Part 1 for the first 75 trials and Part 2 for the last 75 trials). See Table 3 for abbreviations.

Figure S5. (a) Example of one derivation located in the SMA in patient 3 in which post-interval activity was predicted by the target interval (TI) duration and by the TI-duration presented in the prior trial (3 or 7 s). (b) Example of one derivation located in the MCC in patient 3 in which post-interval activity was predicted by the target interval (TI) duration and

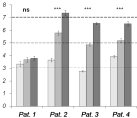
predicted inter-trial variations of the *RI/TI ratio*. High and low *RI/TI ratios* correspond to *RI/TI ratios* which are respectively below and above the median measured separately for each TI-duration. The seven time windows (tw1 to tw7) have a length of 400 ms and are defined between 0.2 and 3 s. See Table 3 for abbreviations and for the definitions.

Figure S6. ICNV-like component time-locked to the 7s target interval (TI) whose amplitude was modulated by the duration presented in the prior trial. The fifteen time windows of (tw1 to tw15) have a length of 400 ms and are defined between 1 and 7 s. See Table 3 for abbreviations.

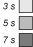
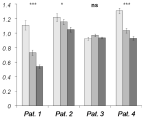
Time reproduction task

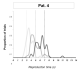
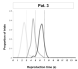
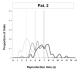
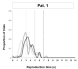


5a
Reproduction time (s)



5b
RUTI ratio



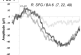
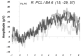


Pat. 1

Sa

Sa

Sa

Pat. 2**Pat. 3****Pat. 4**

Time (min)

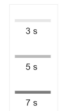
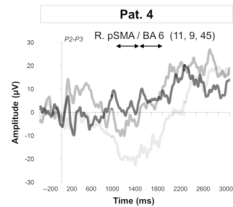
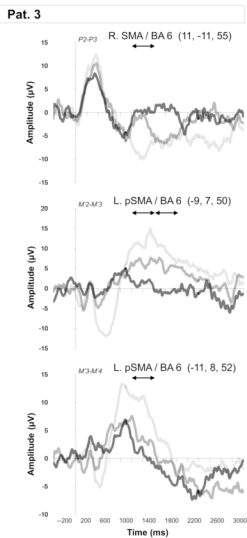
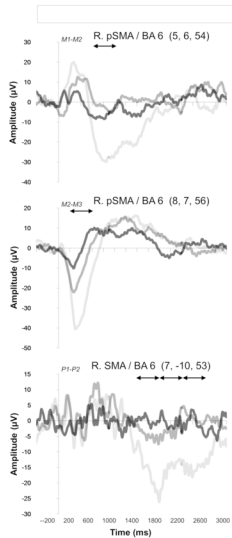
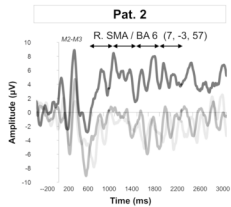
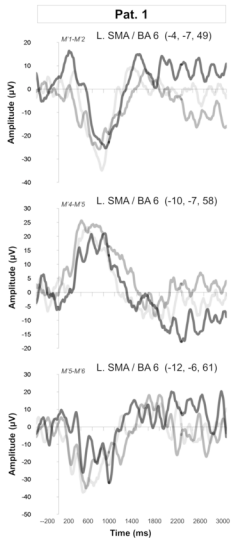


Fig. 3

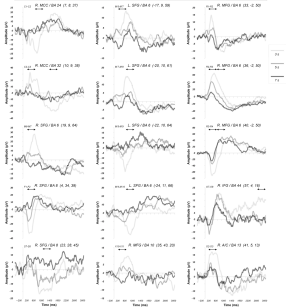


Fig. 3

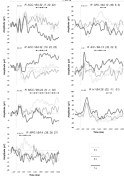
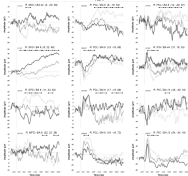
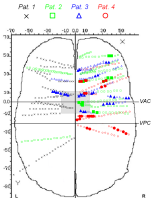
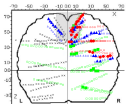
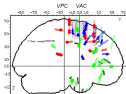
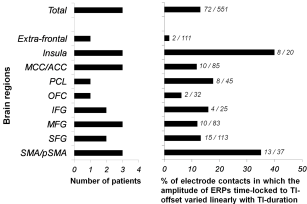


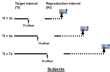
Fig. 4





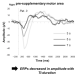


Time reproduction task



Four patients (one female, 32 ± 11.8 years) undergoing BECC stimulation for refractory partial epilepsy with electrodes in the supplementary or pre-supplementary motor area.

Intra-epileptic EEPs time-locked to TI offset



Localization of the effect



IFC: inferior frontal gyrus; MFC/MIF: middle supplementary/middle frontal gyrus; PCL: middle frontal gyrus; CFC: cingulate gyrus; PFC: precentral gyrus; SPC: supplementary gyrus; MIP/MIF: middle supplementary and pre-supplementary motor area.